CHAPTER 4

RESULTS AND DISCUSSION

PART I

0-3 Connectivity cement-based piezoelectric ceramic composite

This chapter focuses on microstructure and electrical properties such as phase formation, dielectric, ferroelectric and piezoelectric properties of cement-based piezoelectric ceramic composite. Material properties of cement-based piezoelectric ceramic composite were investigated. The microstructure constituent and interfacial zone of composites are described. The relationship on electrical and microstructure is discussed in details.

4.1 Phase formation

The XRD patterns of 0–3 lead zirconate titanate (PZT) and Portland cement (PC) composites are shown in Fig. 4.1. XRD patterns of PZT–PC composites are mainly attributed to PZT perovskite phase (2θ = 22.0238, 31.3878, 38.2838, 44.9178 and 55.5248) and the intensities of the peaks increased with increasing PZT content in composite. Furthermore, the amorphous characteristics of the composites can also be observed from the broad peak presented in the XRD patterns.

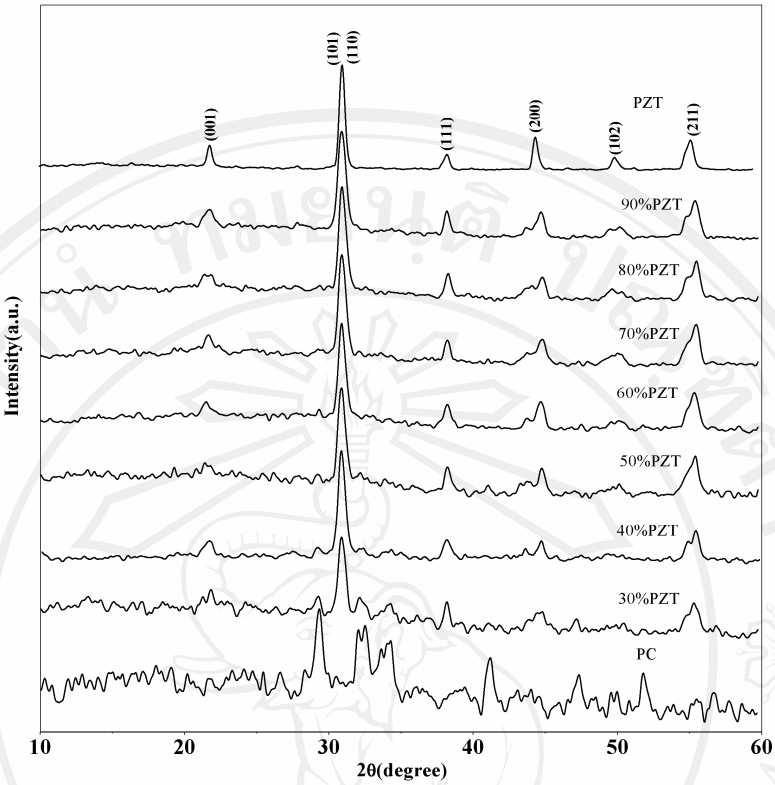

Fig 4.1 XRD pattern of PZT-PC composites

4.2 Dielectric properties

4.2.1 Effect of ceramic piezoelectric content

The dielectric properties of lead zirconate titanate, PZT and Portland cement (PC) with *x*PZT-*(1-x)*PC (where *x* = 0.3, 0.4, 0.5, 0.6, 0.7, 0.8, 0.9 and 1.0) composites were investigated. The dielectric properties of the both composites are measured as a function of content of ceramic piezoelectric (PZT) has been studied at frequency for 1 kHz at room temperatures. It can be seen from Fig. 4.2(a) that there is a roughly nonlinear increase of the dielectric constant values of the composites as a function of the PZT content. It can also be explained that with increasing the PZT volume fraction, the dielectric value of the composite increased gradually.

The reason is probably that the larger the volume fraction of piezoelectric ceramic, the larger the contribution of the piezoelectric ceramic and interface polarization on the total polarization of the composite, which leads to an increase of the dielectric value of the composite. This means that the change of the dielectric constants of the composites is mainly caused by interface polarization of the composites and various polarization of the cement matrix.

Moreover, the enhancement in ε_r value can be attributed to the introducing of PZT content which with high dielectric constant of cement-based composite. PZT piezoelectric exists in the composites as tiny grains, just as introduces a lot of tiny capacitors. The more PZT content, the more tiny capacitors introduced. Therefore, the higher dielectric constant appears in the composites with higher content of the PZT piezoelectric ceramic.

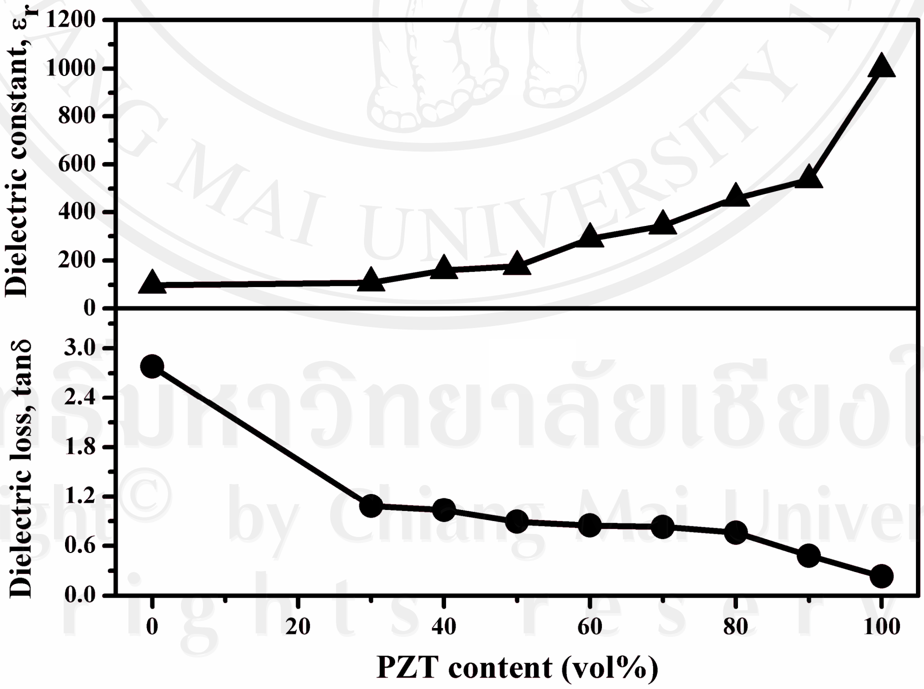

Fig 4.2 Effect of PZT content on dielectric constant and dielectric loss of PZT-PC composite

On the other hand, the dielectric loss results (Fig. 4.2 (b)) were found to decrease with increasing ceramic piezoelectric (PZT) content due to loss cement being used. Conduction ion in the cement matrix would contribute to the loss in the dielectric. A reasonably low *tan δ* value was obtained for composite with high ceramic disperse phase content. In addition, the comparision of experimental results and theoretical values (sum properties as series and parallel; R.E.Newnham (Fig. 4.3(a) and (b)) [58] and cube model; Furukawa principle (Fig 4.3(c))[76]) for dielectric constant of composite with different PZT volume fraction are shown in Fig 4.3. The theoretical values are based on:

Parallel model $$\varepsilon_C = v_1\varepsilon_1 + v_2\varepsilon_2 \tag{4.1}$$

Series model $$\varepsilon_C = \frac{\varepsilon_1 . \varepsilon_2}{v_1\varepsilon_2 + v_2\varepsilon_1} \tag{4.2}$$

Cubic model $$\varepsilon_C = \frac{\varepsilon_1 \cdot \varepsilon_2}{(\varepsilon_2 - \varepsilon_1)\cdot v_1^{-1/3} + \varepsilon_1 \cdot v_1^{-2/3}} + \varepsilon_2 \cdot \left(1 - v_1^{2/3}\right) \tag{4.3}$$

Where ε_C = the dielectric constant of the composites

ε_1 and ε_2 = the dielectric constant of the ceramics and the cement phase

v_1 and v_2 = the volume fraction of the ceramics and the cement phase

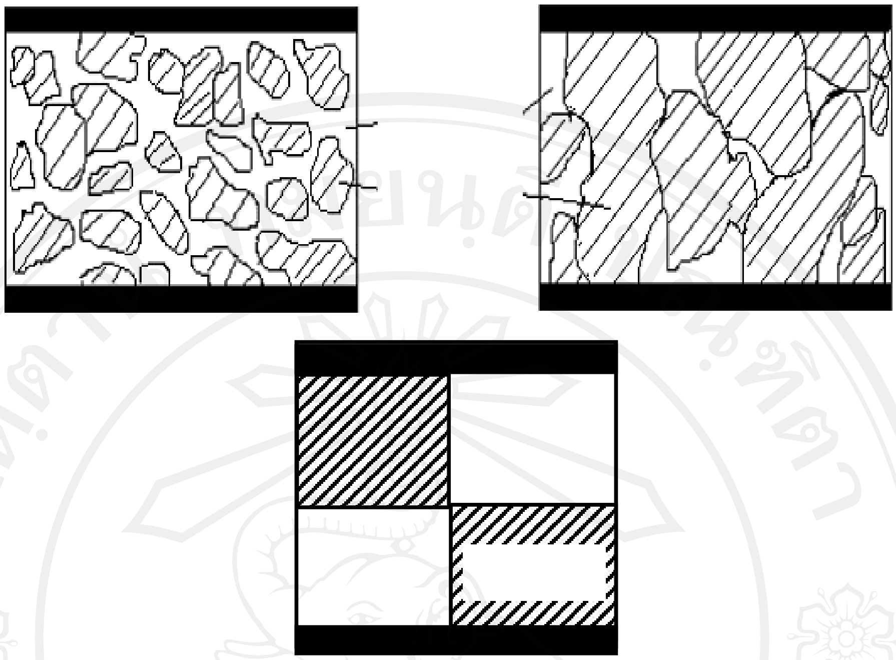

Fig 4.3 Model of composite (a) Series model; (b) Parallel model; (c) Cube model

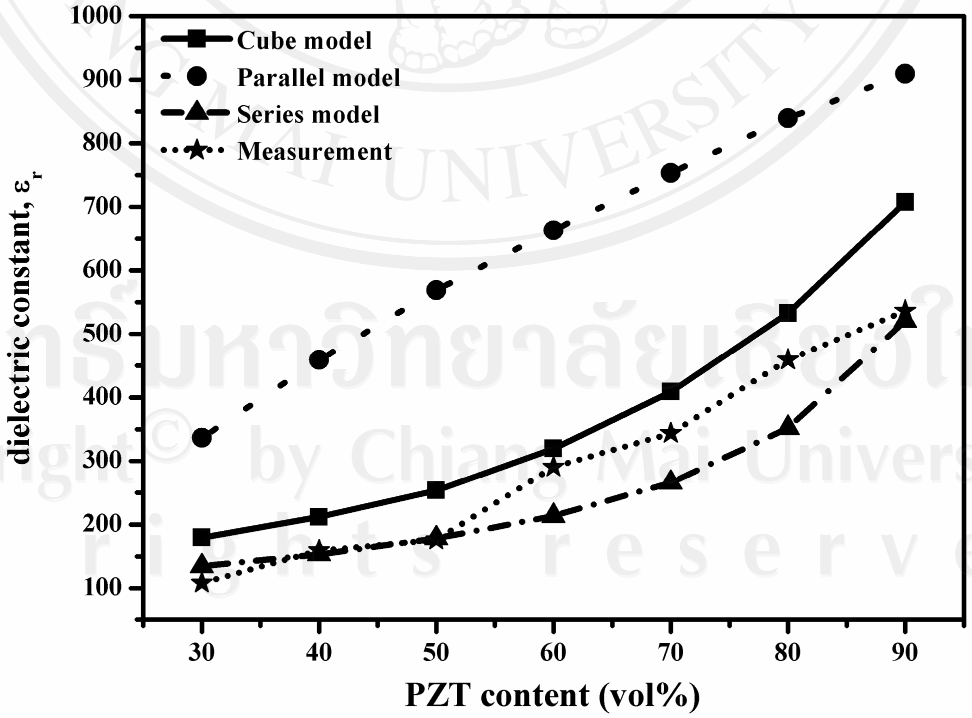

Fig 4.4 Relative dielectric constant versus PZT ceramic content

In the calculation, it is assumed that the polarization of PZT particle is saturated. From Fig. 4.4, it is clear that parallel model and series model are the upper limit and lower limit for relative dielectric constant, respectively. Moreover, the experimental data are close to the theoretical value of the cube and series model for the PZT particle which means the PZT particles in the composites are well dispersed [7].

4.2.2 Effect of particle size of ceramic piezoelectric

Figure 4.5 shows the effect of particle size on dielectric constant *(ε_r)* and dielectric loss *(tanδ)* of the PZT /cement composite at 50 percentages by volume of ceramic. It can be seen clearly in Fig. 4.5 that with increasing PZT particle size, the dielectric constant also increases.

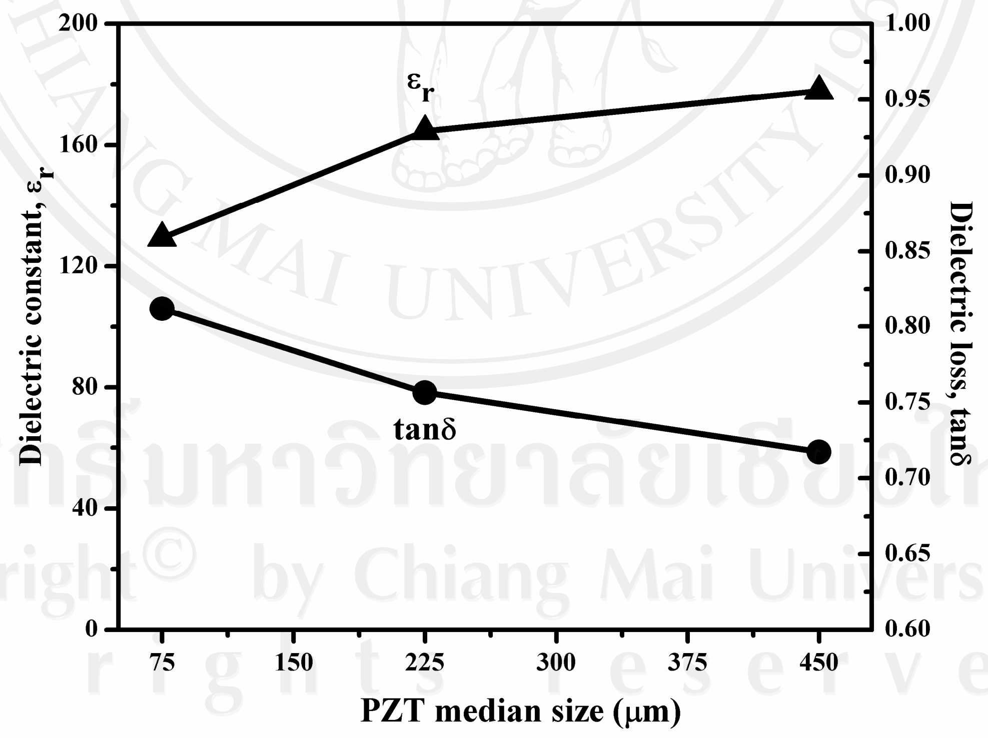

Fig 4.5 Effect of particle size of PZT on dielectric constant and dielectric loss of PZT-PC composite

It could be explained by the inferior effects of the interface between PZT and cement and poor crystalline structure of the PZT that would increase with smaller particle size. Furthermore, the dielectric loss decreased for the composite with a higher PZT particle size as shown in Fig 4.5.

4.3 Piezoelectric properties

In this part ceramic piezoelectric as PZT was used for fabrication for piezoelectric PZT-cement composites. Effects on piezoelectric properties such as effect of particle size, effect of PZT content, effect of aging and the degree of poling (which a critical factor in the piezoelectric properties and is often restricted by character of each component phase of the composites) are reported.

4.3.1 The degree of poling

Effect of poling temperature

In this subtopic, the effect of poling temperature on the piezoelectric properties such as piezoelectric coefficient (d_{33}) of 0-3 connectivity PZT- Portland Cement (PC) composites was investigated. PZT-PC composites were produced using PZT of 50% by volume and the poling temperatures were selected at 100°C, 130°C and 160°C respectively. In order to investigate the influence of the poling temperature, samples were polarized under poling field E at 1.0 kV/mm and poling time t at 45 min. It can also be observed that if the poling field continually increases, samples have a high chance of breaking down. This is due to the presence of some matrix pores, particle pores and interface pore in the composites. The pores are made up of gel pore and capillary. There is some water in pores, which greatly lowers the resistivity and gives rise to the leakage current in the course of the poling [15, 84] .

The dependence of the d_{33} on poling temperature is shown in Fig. 4.6. It can be seen that the value of d_{33} of the poling temperature at 130°C (d_{33}=13 pC/N) was found to be higher than the d_{33} values of the poling temperature at 100°C (d_{33} = 9 pC/N). It is predicted that the d_{33} increases remarkably as the poling temperature increases until 130°C. However, when the poling temperature exceeds 160°C the d_{33} values (d_{33} = 5 pC/N) were lowest. In general, the higher the poling temperature is the better the piezoelectric property of the composites. However, for Portland cement based piezoelectric composite, if the poling temperature is higher than 130°C, the main hydrated products of the Portland cement, such as CSH, ettringite would lose a large amount of crystal. This would change the crystal structure of Portland cement matrix and finally result in degeneration of the composites properties.

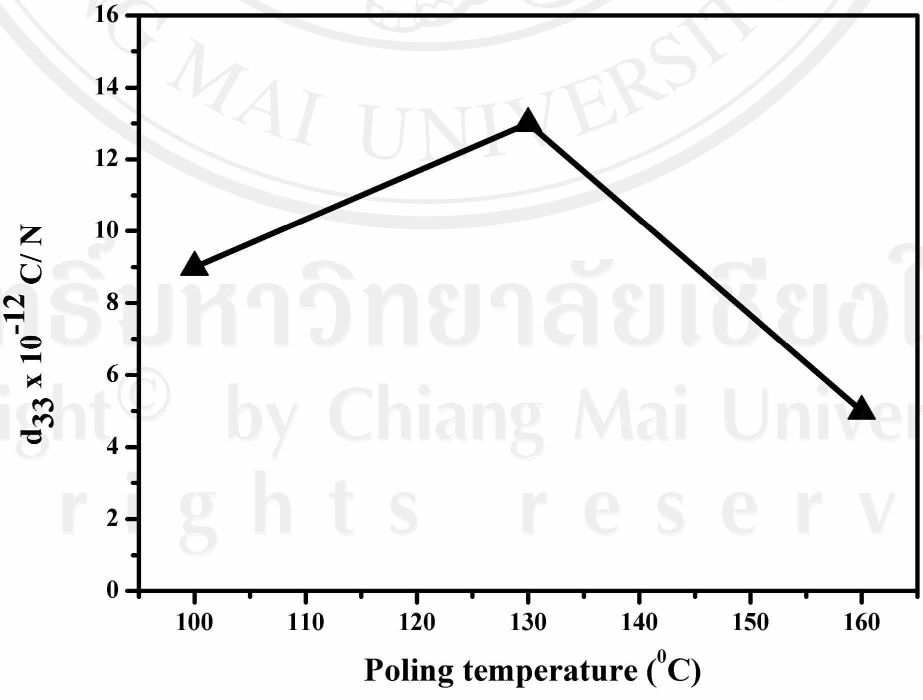

Fig 4.6 Relationship between the d_{33} and the poling temperature

In addition, there are ions, such as Ca^{2+}, OH^- and Al^{3+} in the Portland cement matrix [7, 78]. As the poling temperature increases ions migration takes place leading to a rise of conductivity and also affected d_{33} because the ions in the cement matrix lead to a rise of leakage current which decrease the piezoelectricity. Therefore, 130°C is chosen as the optimum poling temperature in this work.

Effect of poling time

PZT-PC composites were produced using PZT of 60% by volume. The relationship between the d_{33} values and poling time under the same poling field (1kV/mm) and poling temperature (130ºC) is shown plotted in Fig. 4.7. The effects of poling time of 15, 30, 45, 60 and 90 minutes were studied.

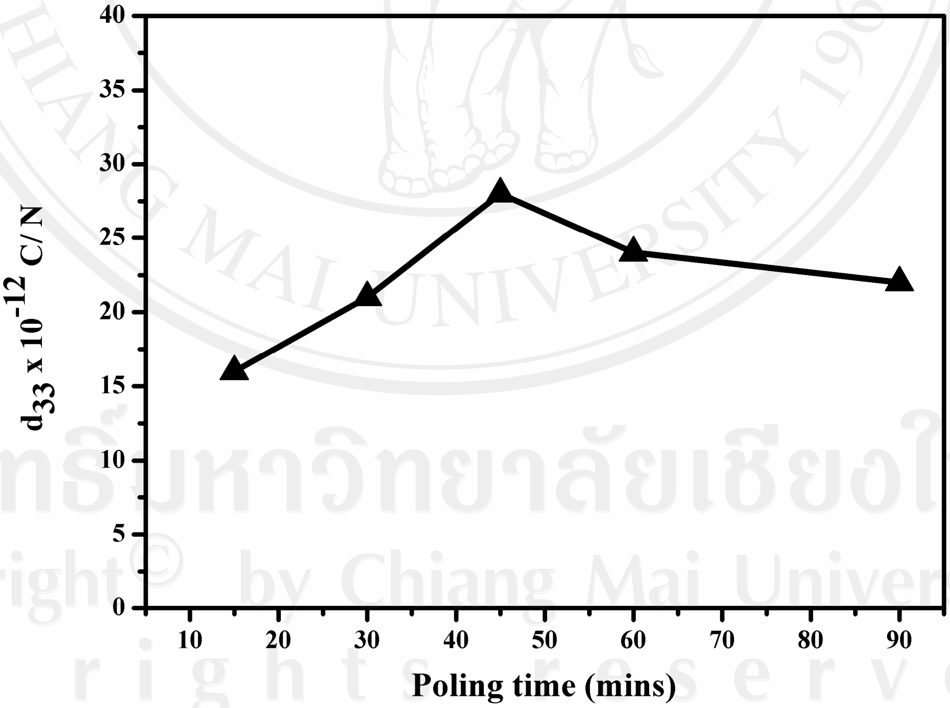

Fig 4.7 The effect of poling time on the piezoelectric coefficient (d_{33})

It can be seen that the value of d_{33} for the composite sample poled for 45 minutes (d_{33}= 28pC/N) was found to be highest when compared to d_{33} values of samples poled for 15 or 90 minutes where d_{33} values were measured at 16 pC/N and 22 pC/N respectively.

From Fig 4.7, in the part of discussion, the values of the d_{33} increases remarkably with increasing the poling time in the initial period of poling and highest at 45 min. This is due to the reversal of the 180° ferroelectrics domain takes place mainly at the initial stage of poling which cannot give rise to local stress and is performed in short time. Nevertheless, the reversal of 90° ferroelectrics domain plays an important role, which is attended by producing of the local stress and strain. This means that it is not easy to make the 90° ferroelectrics domain reversal [15, 80]. Therefore, the degree of poling can be improved by extending the poling time up to 45 min.

4.3.2 Effect of PZT content on piezoelectric properties

PZT-PC composites of 0-3 connectivity were produced using PZT of 30-90 % by volume. The variation of piezoelectric constant as a function of content of PZT were studied under the same poling field (2kV/mm), poling time (45 mins) and poling temperature (130ºC) and the results of piezoelectric constant (d_{33}) of the composites were plotted in Fig. 4.8 against PZT content with the theoretical curves of different models (series model, parallel model and cubes model). From Fig. 4.8, it can be seen that these is a nonlinear increase of the d_{33} values of the composites as a function of the PZT content. Also, it can be easily understood that as a functional phase in the composites, higher PZT ceramic content is beneficial to the piezoelectric performance of 0–3 type cement-based PZT composites. The experimental results confirm that the polarizing behaviors of the 0–3 type cement-based PZT composites can be well described by the series model. The theoretical equations of series, parallel and cubes model for the relative dielectric constant (ε_r) and piezoelectric strain factor (d_{33}) in two-phase systems are as following [58, 76, 78]:

Parallel model
$$^{C}d_{33} = \frac{^{1}v.^{1}d_{33}.^{2}S_{33} + ^{2}v.^{2}d_{33}.^{1}S_{33}}{^{1}v.^{2}S_{33} + ^{2}v.^{1}S_{33}} \qquad [58] \qquad (4.4)$$

Series model
$$^{C}d_{33} = \frac{^{1}v.^{1}d_{33}.^{2}\varepsilon_{33} + ^{2}v.^{2}d_{33}.^{1}\varepsilon_{33}}{^{1}v.^{2}\varepsilon_{33} + ^{2}v.^{1}\varepsilon_{33}} \qquad [76] \qquad (4.5)$$

Cubic model
$$^{C}d_{33} = {}^{1}d_{33}.\frac{^{1}v}{^{1}v^{\frac{1}{3}} + \left(1 - {}^{1}v^{\frac{1}{3}}\right).\frac{^{1}\varepsilon_{33}}{^{2}\varepsilon_{33}}}.\frac{1}{1 - {}^{1}v^{\frac{1}{3}} + {}^{1}v} \qquad [78] \qquad (4.6)$$

Where $^{C}d_{33}$ = the piezoelectric constant of composite

$^{1}d_{33}$ and $^{2}d_{33}$ = the piezoelectric constant of the PZT and the cement phase

$^{1}\varepsilon_{33}$ and $^{2}\varepsilon_{33}$ = the dielectric constant of the PZT and the cement phase

$^{1}S_{33}$ and $^{2}S_{33}$ = the elastic compliance of the PZT and the cement phase

^{1}v and ^{2}v = the volume fraction of the PZT and the cement phase

However, it should be noted that it would become very difficult to produce sample greater than 90% PZT volume since there would not be enough binder (cement) to bind the composite together. Above all, the results have shown that it is possible to produce piezoelectric-cement based composite at up to 90% PZT by volume and these composites can become piezoelectric so long as the composites (i.e. PZT in the composites) were subjected to successful poling

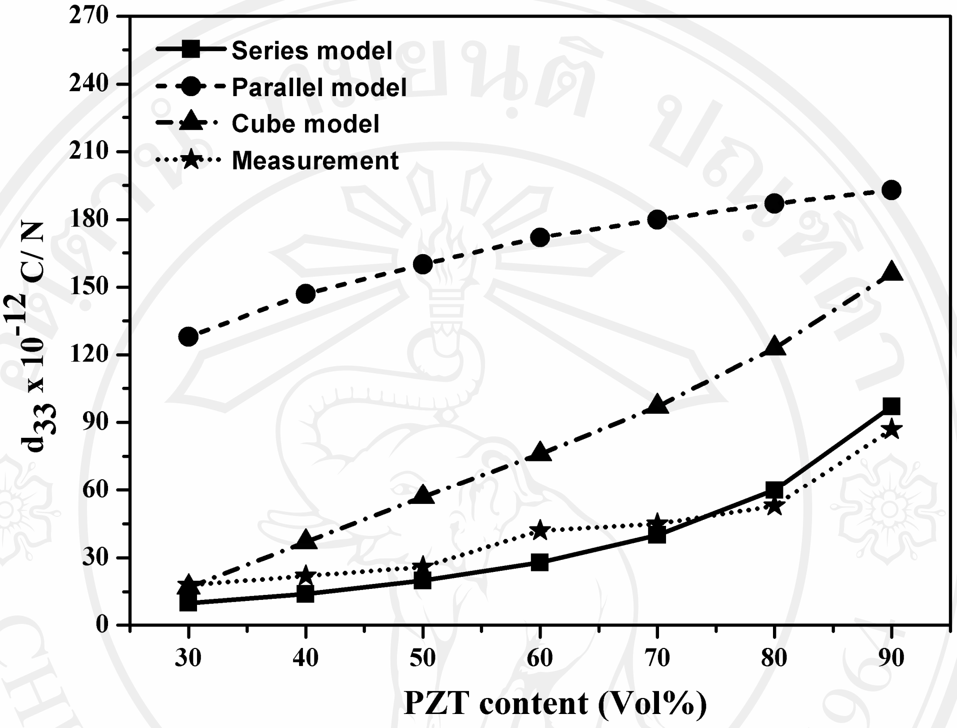

Fig 4.8 The effect of PZT content on the piezoelectric coefficient (d_{33})

4.3.3 Effect of PZT particle size on piezoelectric properties

The effect of PZT particle size on the piezoelectric properties of PZT–PC composites was investigated. PZT of various median particle sizes (4-450 μm) were used at 50% by volume to produce the composites. The composites were poled under the same poling field (2kV/mm), poling time (45 mins) and poling temperature (130ºC). After successful poling, the piezoelectric constant (d_{33}) values were measured. The effect of PZT particle size on the d_{33} value can be seen in Fig.4.9.

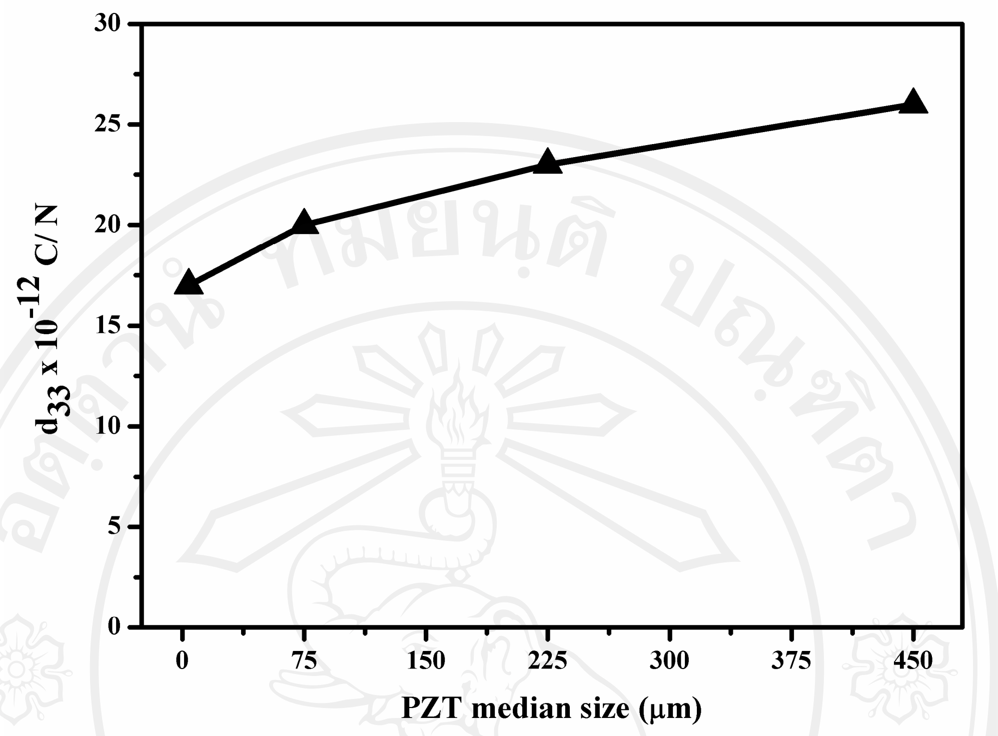

Fig 4.9 The effect of PZT particle size on the piezoelectric coefficient

It is clearly seen that with an increase in PZT particle size, d_{33} values became higher and it is again clear that the highest value was found when the composites were made using the largest PZT particle size (d_{33} = 26 pC/N). This is due to the fact that contact surfaces between cement matrix and PZT particles became less when larger PZT ceramic particle was used, thus bringing out the optimum piezoelectricity in the 0-3 PZT cement composites [93]. The highest optimum value of d_{33} obtained was therefore found in the composite with PZT particle size of 450 μm. This is because that the large particles, which leads to a larger electric field acting on the ceramic giving a greater remnant polarization of the ceramic phase than composites prepared with smaller particles [80, 84].

4.3.4 Effect of hydration ages on piezoelectric properties

The effect of hydration age of the Portland cement on the piezoelectric constant d_{33} with 30-100 Vol% of PZT content is shown in Fig. 4.10. The composites were poled at 130°C for 45 min at poling field of 2kV/mm. From Fig. 4.10 (a), at the period of 10 days the d_{33} values can be seen to be separated into 3 groups i.e. group *A* are 30, 40, 50% PZT, group *B* are 60, 70, 80%PZT and group *C* is 90%PZT respectively. It can be seen that before 90 days, the d_{33} value of piezoelectric composites increase at a faster rate as the hydration age increases especially in group *A* (Fig. 4.10 (b)) and increase at a slower rate as the hydration age increases in group B and *C* (Fig. 4.10 (c)). After that, when the hydration age of cement reaches 1 year, the d_{33} tends to be stable as well as shown in Fig 4.10(d).

The phenomenon that the piezoelectric performances of piezoelectric composites change with age after the poling is usually called the aging phenomenon. At the early stage of the hydration process, there are usually some big pores in the cement matrix. Moreover, the interfaces between the cement matrix and the piezoelectric ceramic particles are not perfect, some interfacial cracks have been observed (see SEM micrograph, Fig 4.14). These pores and interfacial cracks remarkably decrease the local stress applied on PZT particle, resulting in a smaller d_{33} value. With the increase of cement hydration ages, the porosity in the cement matrix remarkably decreases, accompanying with increase volume expansion at the same time, leading to a better combination between the piezoelectric ceramic particles and the cement matrix. In this case, the external strain can be transferred to the piezoelectric ceramic particles effectively. Therefore, the local stress increases continuously and d_{33} increases which period of cement hydration ages [85].

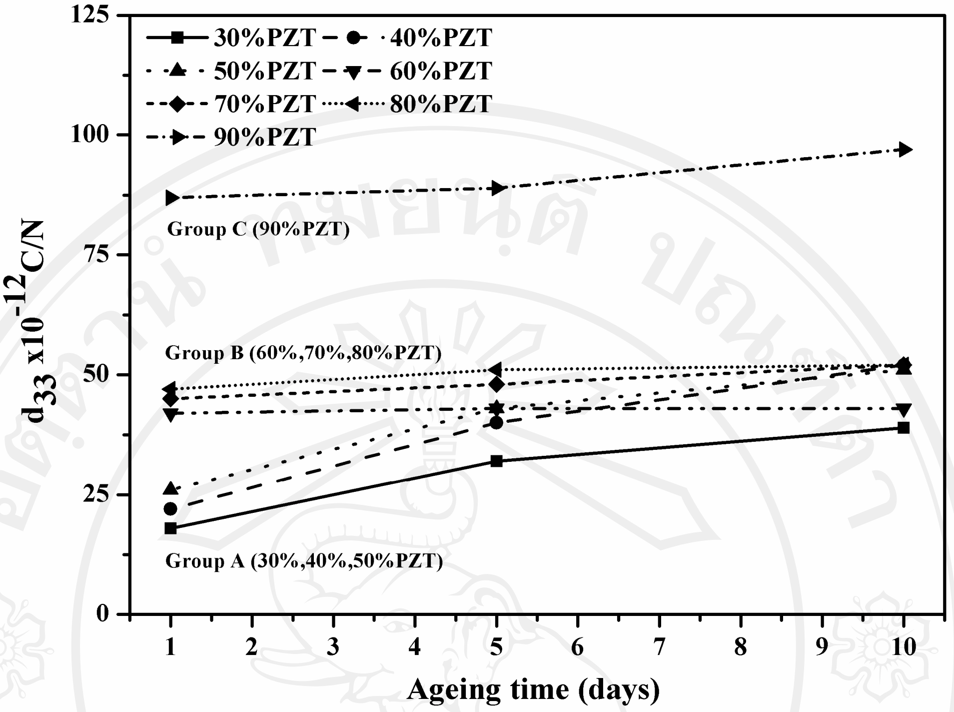
30%PZT
40%PZT
50%PZT
60%PZT
70%PZT
80%PZT
90%PZT
Group C (90%PZT)
Group B (60%,70%,80%PZT)
Group A (30%,40%,50%PZT)
d_{33} x10^{-12}C/N
Ageing time (days)
0
25
50
75
100
125
1
2
3
4
5
6
7
8
9
10

(a)

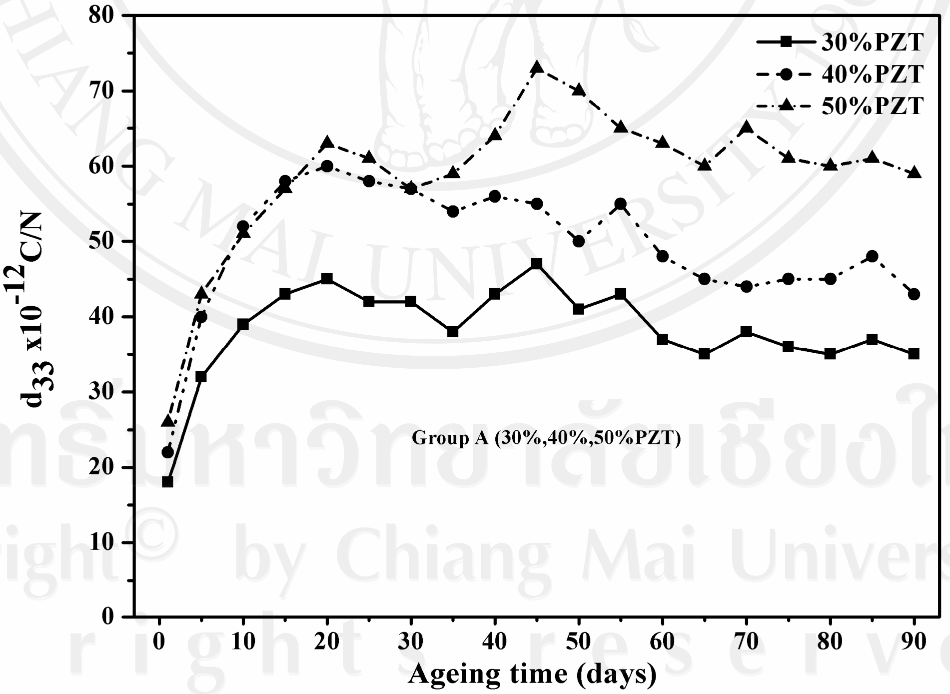
30%PZT
40%PZT
50%PZT
Group A (30%,40%,50%PZT)
d_{33} x10^{-12}C/N
Ageing time (days)
0
10
20
30
40
50
60
70
80
0
10
20
30
40
50
60
70
80
90

(b)

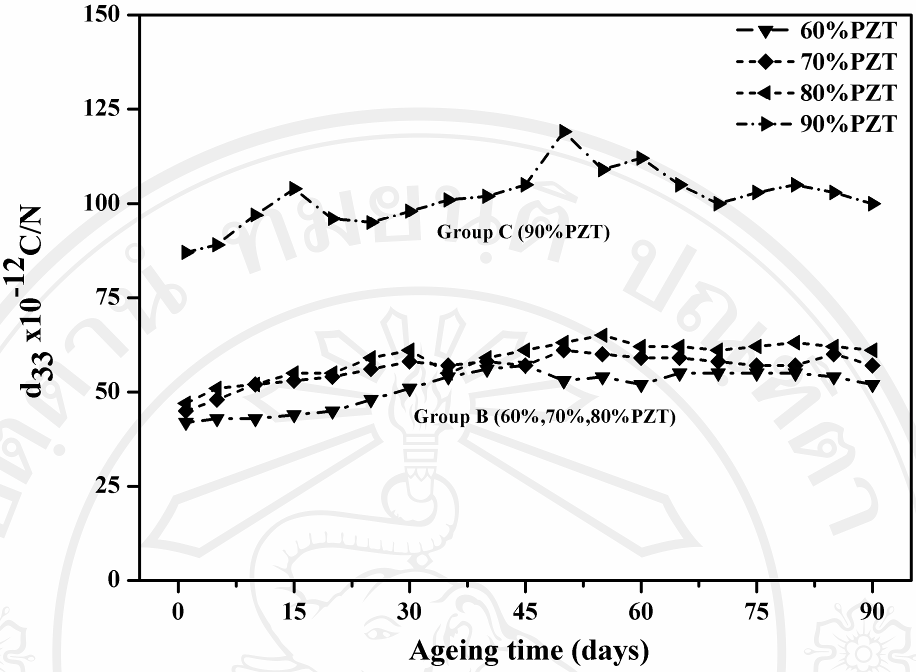

(c)

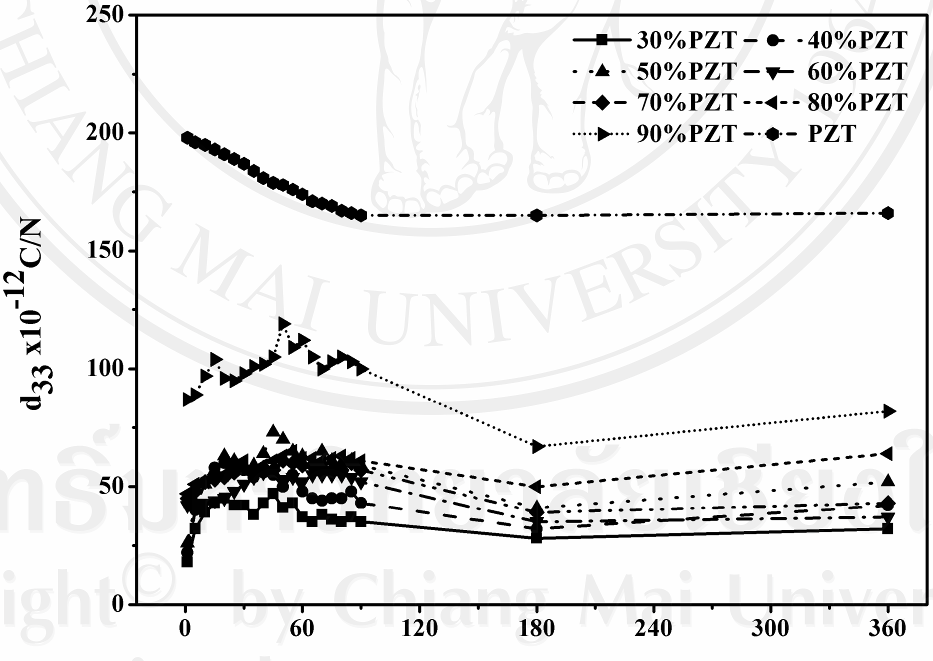

(d)

Fig 4.10 The effect of hydration age on the piezoelectric coefficient (d_{33}) of composite for (a) 10 days; (b) 90 days of 30,40,50%PZT; (c) 90 days of 60,70,80,90%PZT; (d) 1 year.

4.4 Ferroelectric properties

In this part the effects of the frequency and electric field on the ferroelectric polarization-electric field (*P-E*) hysteresis of the PZT-cement composites were investigated. In addition, the ferroelectric properties were investigated as various PZT content on ferroelectric hysteresis *(P-E*) loops at room temperature for all composites.

4.4.1 Ferroelectric hysteresis behavior in 0-3 ceramic-cement composites: Effects of frequency and electric field

PZT ceramic particles were mixed with Portland cement (PC) to produce 0-3 connectivity PZT-PC composites of 50:50 by volume. The effects of the frequency and electric field on the ferroelectric polarization-electric field (*P-E*) hysteresis of the composites were investigated.

It can be seen from Fig. 4.11(a) that when the composite was subjected to different electric field, the *P-E* hysteresis loops can be seen at different electric field. It must first be noted that all ferroelectric hysteresis loops (*P-E* loops) of the PZT-cement composites show a "*lossy*" feature with round tips as a result of cement matrix in the composites. It is believed that when an external electrical field acts on the cement matrix many weak conducting ions such as Ca^{2+}, OH^{-}, Al^{3+} begin to migrate besides the polarization of electron. These ions cause higher conducting loss in the composites, hence a lossy feature is then observed in all the *P-E* loops obtained [86]. However, this study primarily aims at comparing the effects of the frequency and amplitude of the applied electric field on the hysteresis behavior, as reported in PZT ceramics and other monolithic materials [94-96]. Therefore, the ferroelectric parameters obtained here are used exclusively for comparison purpose among themselves. One can define two parameters based on the *x*- and *y-axes* intercepts.

With a lossy behavior, it is impossible to achieve the fully saturated loops, hence the typical hyteresis parameters; i.e. the remnant polarization (P_r) and the coercive field (E_c) cannot be extracted. For comparison, we define the y-axis intercept at a given applied field as the "*instantaneous*" remnant polarization (P_{ir}), while the x-axis intercept is called the "*instantaneous*" coercive field (E_{ic}). From Fig. 4.11(a), an increase in the amplitude of the field E_0 makes the loop larger and increases its angle to the E axis of inclination. Furthermore, it can be seen that there is an increase in the so called "*instantaneous*" remnant polarization (P_{ir}) and the "*instantaneous*" coercive field (E_{ic}) which represents the polarization at zero field and electric field at zero polarization at each measured frequency and E_0.

At frequency of 60 Hz, P_{ir} and E_{ic} can be seen to increase for the hysteresis loops with the electric field of 10kV/cm to 25kV/cm, respectively. The increase in both the "*instantaneous*" parameters is due to the electric charge in a polar material when induced with increasing an external electric field. Previous investigations on the ferroelectric hysteresis behavior of the ferroelectric materials under sub-coercive field condition also showed similar changes of the hysteresis parameters with the applied field [95, 96]. When the hysteresis loops were plotted at 25kV/cm and with varying frequency from 20 to 100 Hz (Fig. 4.11 (b)), a typical hysteresis loops can still be seen at lower frequency (20 and 40 Hz).

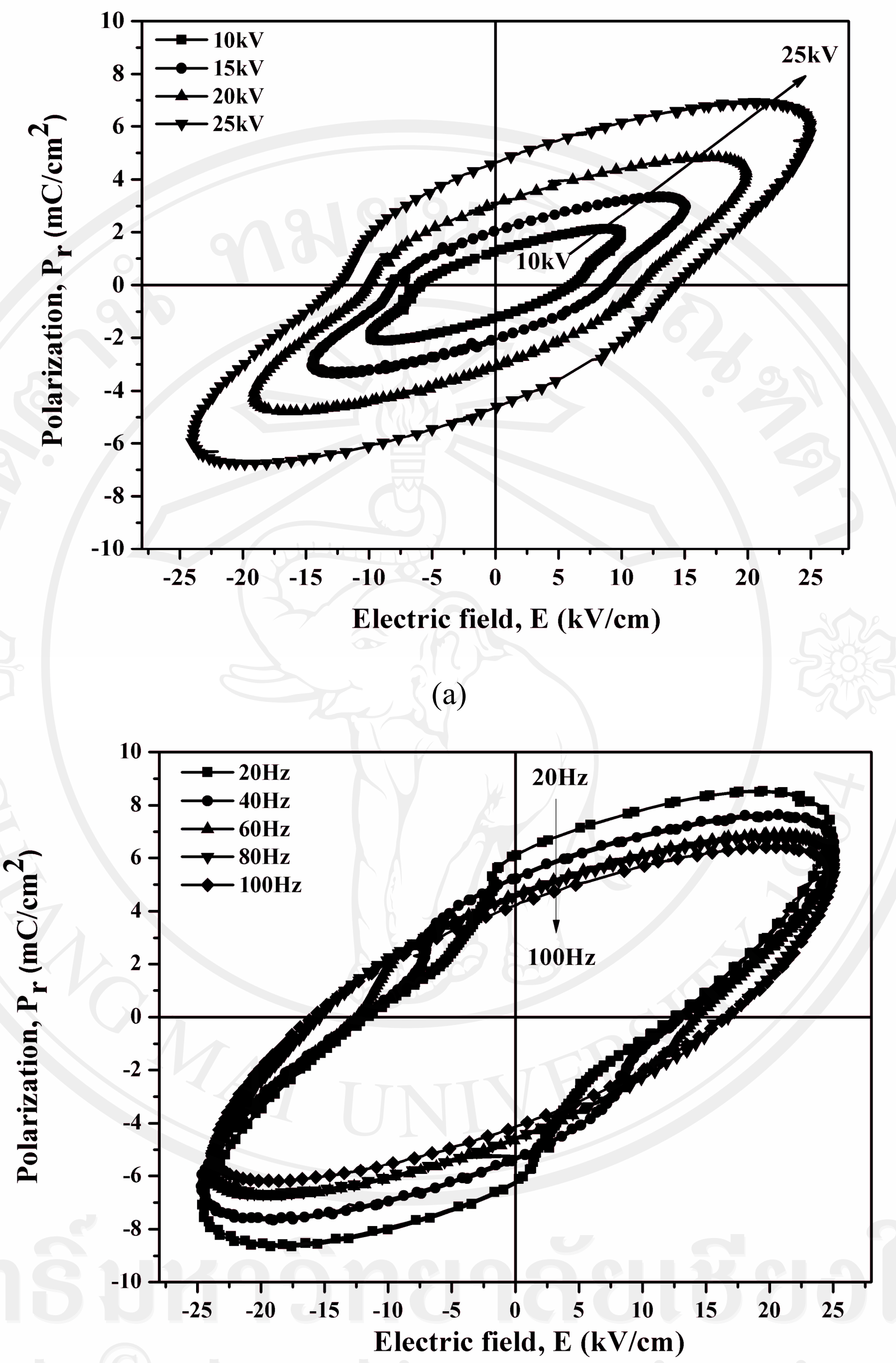

(a)

(b)

Fig 4.11 Effects of electric field (a); and frequency (b); on the ferroelectric (*P*-*E*) hysteresis loops of PZT-PC composites (with fixed *f* of 50 Hz and fixed *E* of 25kV/cm)

However at higher frequency i.e. 100 Hz, the loop tends to stretched out more and the loop no longer resemble a typical hysteresis. The "*instantaneous*" remnant polarization (P_{ir}) and "*instantaneous*" coercive field (E_{ic}) can be seen to decrease with an increase in frequency. The observation that the P_{ir} and E_{ic} decreases with increasing frequency is ascribed to the delayed response of the polarization reversal to the varying external field. Similar behavior was observed in previous study on ferroelectric ceramics [97-99].

It should be noted here that a loss from the cement can be seen to be more sensitive at higher frequency especially at 100 Hz where an oval shaped typical of a resistance is seen. It is understood that at the high frequency the interfacial polarizations cannot follow the change of the electric field due to the longer time taken for the space charge polarization to occur [95]. It is believed that when an external electrical field acts on the cement matrix many weak conducting ions such as Ca^{2+}, OH^{-}, Al^{3+} begin to migrate besides the polarization of electron. These ions move slowly when it reaches the interface of PZT and cement or in the defect areas and there is an accumulation effect which in turn results in the polarization of a space charge, and at lower frequency all the polarization can follow these changes of electrical field [86].

4.4.2 Effects of PZT content on ferroelectric hysteresis behavior of 0–3 PZT-Portland cement composites

Lead zirconate titanate (PZT) - Portland cement (PC) composites were produced. PZT amount used in this work was 40%, 50% and 60% by volume. The ferroelectric properties were investigated at various PZT content on ferroelectric hysteresis *(P-E*) loops.

The PZT-PC composites exhibit typical ferroelectric hysteresis (*P–E*) loops at the external electrical field 20 kV and fixed frequency of 20Hz at room temperature as shown in Fig. 4.12. From Fig. 4.12, it can be seen that the PZT volume fraction has a significant influence on the *instantaneous* remnant polarization (P_{ir}) and *instantaneous* coercive field (E_{ic}). With increasing the PZT volume fraction, the *instantaneous* remnant polarization (P_{ir}) and the *instantaneous* coercive field (E_{ic}) increased. It can be explained that the PZT has a strong ferroelectricity when increasing PZT content in the composite, the higher *instantaneous* remnant polarization (P_{ir}) of the composite will be [100].

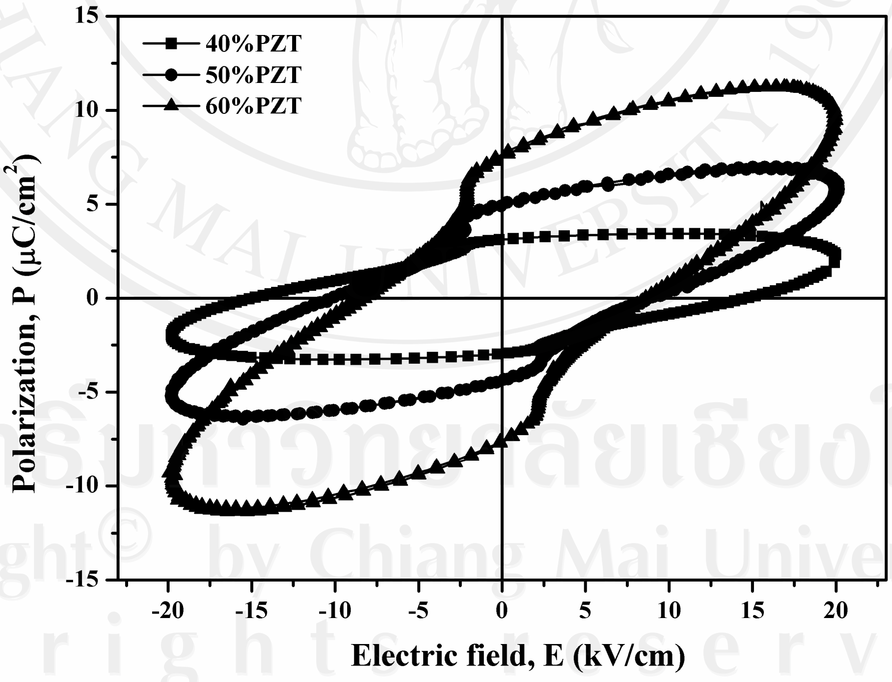

Fig 4.12 Effects of PZT content on the ferroelectric (*P-E*) hysteresis loops of PZT-PC composites (with fixed *f* of 20 Hz) of external electric field amplitude at 20kV/cm

4.5 Interfacial morphology and microstructure

4.5.1 SEM micrograph

Lead zirconate titanate (PZT) and Portland cement (PC) composite were fabricated using 60% of PZT by volume. Scanning Electron Microscope was used to investigate the morphology at the interfacial zone of PZT-Portland Cement composites. Angular PZT ceramic grains were found to bind well with the cement matrix. The SEM images of the PZT-PC composites are shown in Fig. 4.13 where PZT grains can be seen to disperse randomly in the PC matrix (Fig. 4.13 (a)) and is seen to bind firmly with the cement matrix that comprises of calcium silicate hydrates or CSH (Fig. 4.13(b,c)). The angular shape PZT particle is believed to contribute to better mechanical interlocking with the cement paste [101] due to the angular aggregate having rough surface appearing to provide better mechanical interlocking with the cement paste than aggregate that is rounded and smooth.

It can be explained that the PZT particles are well separated in the matrix without much direct contact between particles. The SEM micrograph reveal that a typical microstructure of the composites at the interfacial zone between the PZT ceramic particle and the Portland cement matrix where PZT ceramic grains can be seen next to cement hydration products such as calcium silicate hydrates (CSH), Calcium hydroxide $Ca(OH)_2$ (The SEM micrographs of $Ca(OH)_2$ do not show any specific crystalline form) and Ettringite. Calcium hydroxide and Ettringite is present as a major crystalline phase however, the properties of cement based products are largely dictated by CSH. Hydrated phases, mostly CSH, form slowly and the material consolidates as space is filled with CSH and crystals of Calcium hydroxide and Ettringite phase.

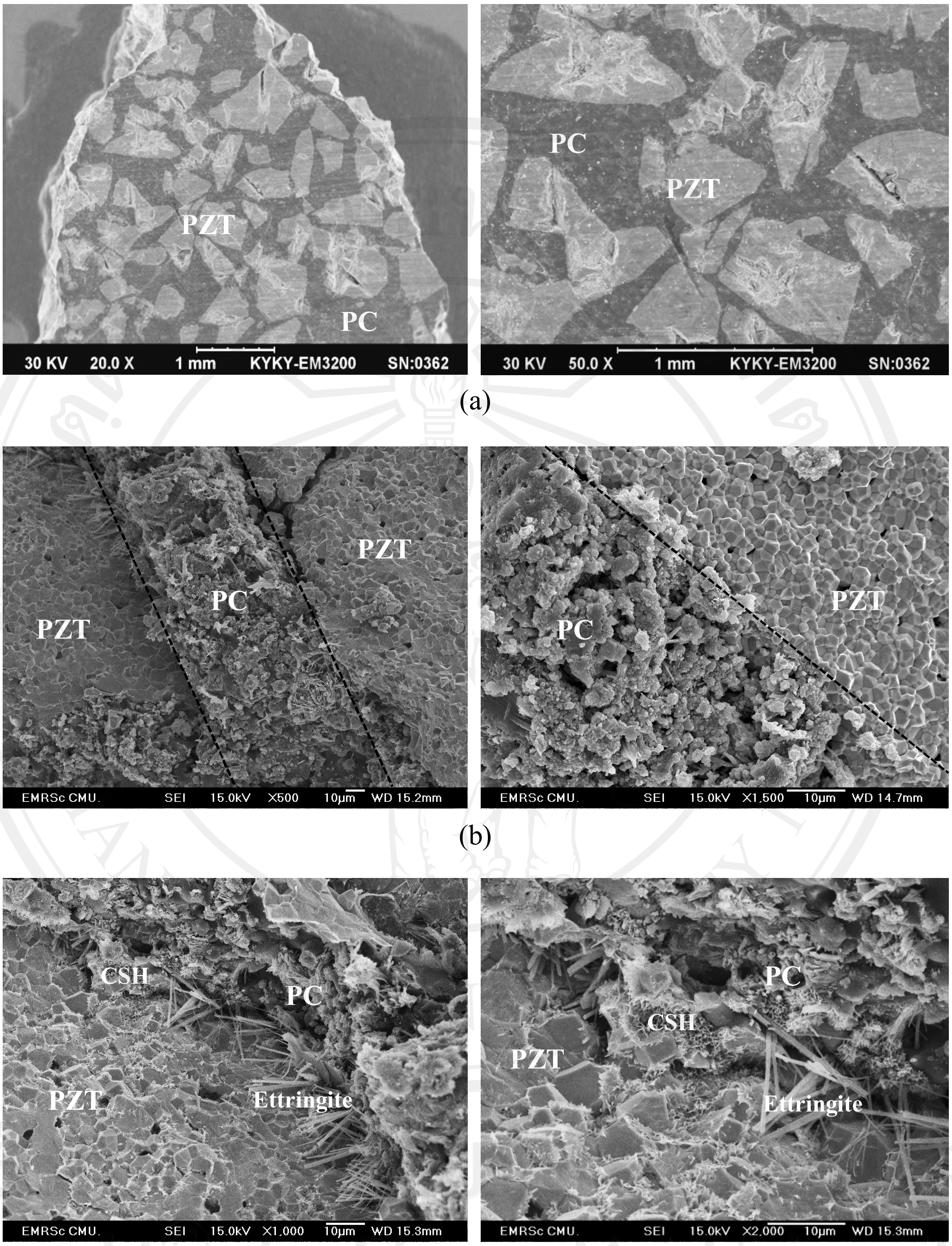

(a)

(b)

(c)

Fig 4.13 SEM micrographs at interfacial zone of PZT-PC composites; (a) magnification 20× and 50×, (b) magnification 500× and 1500× and (c) magnification 1000× and 2000×

Calcium silicate hydrate (CSH) of rather indefinite composition which is mainly amorphous. Moreover, many pores can be found in the interface between PZT particles and cement matrix.

The SEM micrograph at the interfacial zone of the PZT-PC composites are shown in Fig. 4.14(a-b), there are usually some pores in the Portland cement matrix. Moreover, the interfaces between the cement matrix and the piezoelectric ceramic particles or PZT are not perfect, some interfacial cracks have been observed. These pores and interfacial cracks obstruct a stress movement and remarkably decrease the local stress applied on PZT particle, resulting in a smaller piezoelectric coefficient; d_{33} value [85]. Cement paste matrix is a porous material with a complicated microstructure.

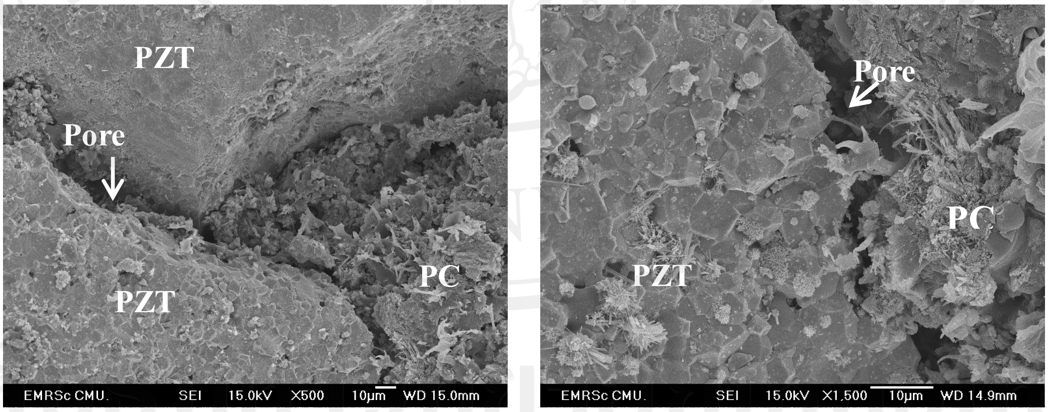

(a) (b)

Fig 4.14 SEM micrographs of PZT-PC composites (a) magnification ×500 and (b) magnification ×1,500

4.5.2 Domain configurations using PFM

Piezoresponse force microscope was used to investigate the morphology and domain configurations at the interfacial zone of PZT-Portland cement composites. Angular PZT ceramic grains were found to bind well with the cement matrix. The submicro-scale domains were clearly observed by piezoresponse force microscope at the interfacial regions between the piezoelectric PZT phase and Portland cement phase, and are clearer than the images obtained for pure PZT. This is thought to be due to the applied internal stress of cement to the PZT ceramic particle which resulted to clearer images.

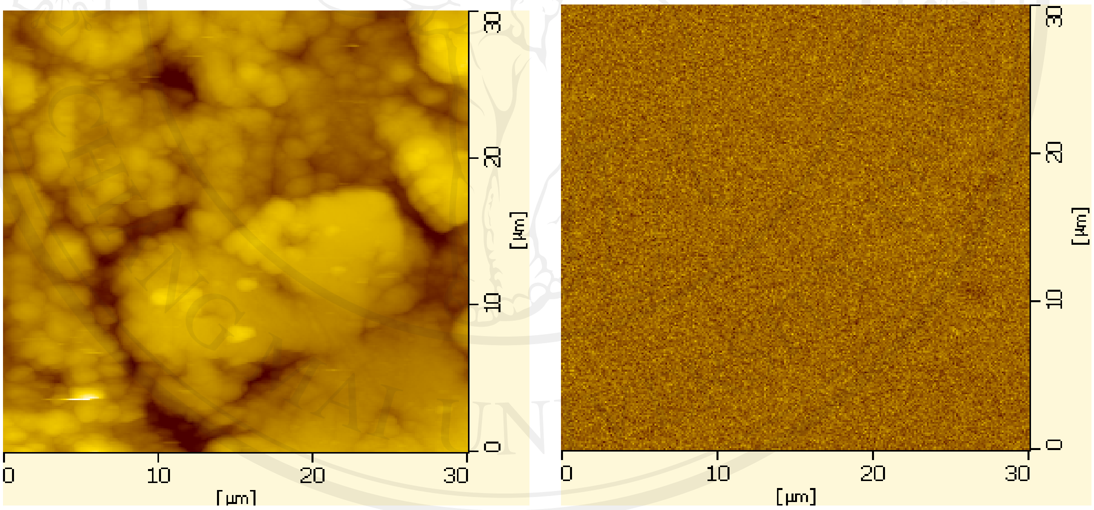

(a) (b)

Fig 4.15 The topography image (a) and the corresponding piezoresponse image (b) for scanning area of 30 x 30μm^2 of Portland cement (PC)

Fig. 4.15 shows a 30 x 30 μm^2 AFM image of cement paste (a), the topography image, and (b), the piezoelectric image. The topography image shows the microstructure of the surface of the cement paste, scanned in a humid air environment at room temperature. The paste is composed of clusters of grains with sizes in the range from 1 to 2 µm. Such a structure is comparable with the description of CSH phase as 'small equant grains' by Diamond [102]. Images of CSH gel are shown by spherical like particles of different sizes in different areas.

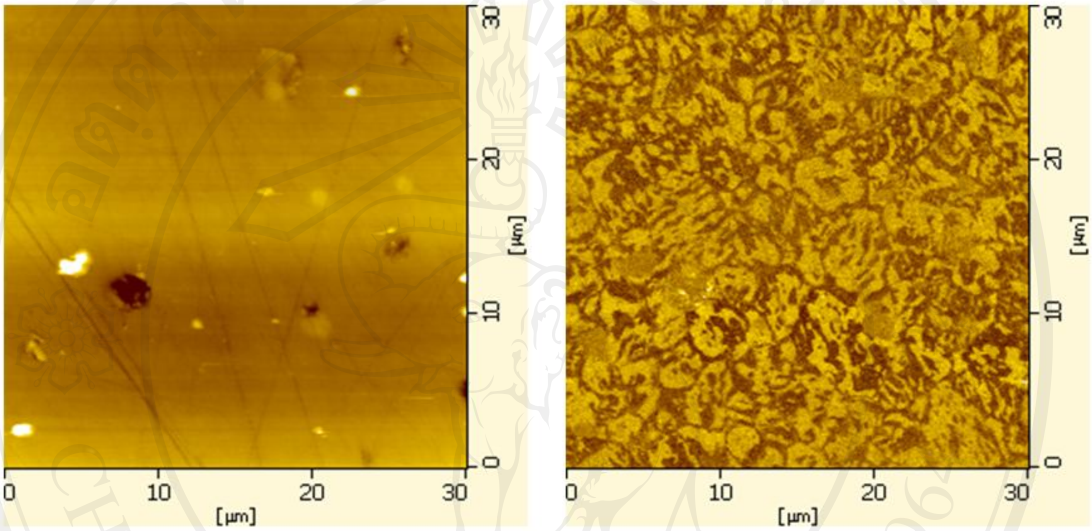

(a) (b)

Fig 4.16 The topography image (a) and the corresponding piezoresponse image (b) for scanning area of 30 x 30μm^2 of Lead zirconate titanate (PZT)

Fig. 4.16(a) and (b) shows the topography and piezoresponse mode images of 10μm x10 μm scanning areas of PZT phase, in which the image voltage has amplitude of 12 V and a frequency of 8 kHz. The piezoresponse images show inhomogeneous domain configurations which agree with the kind of domain morphology reported previously by Zeng *et al.* [91]. According to PFM, domain imaging is based on detecting locally piezoelectric vibration of the ferroelectric domains caused by alternating external field ($V_{ac} = V_0 \sin \omega t$) between the tip and the counter electrode of the sample due to the converse piezoelectric effect. The amplitude and phase of the piezoresponse signal are related to the magnitude of the piezoelectric coefficient and the direction of local polarization, respectively. The irregular bright and dark contrasts regions in Fig. 4.16(b) are found to be antiparallel polarization domains, i.e. 180° domains [92, 102]. So the bright areas in the piezoresponse amplitude image show greater piezoelectricity, the dark areas weaker piezoelectricity [91].

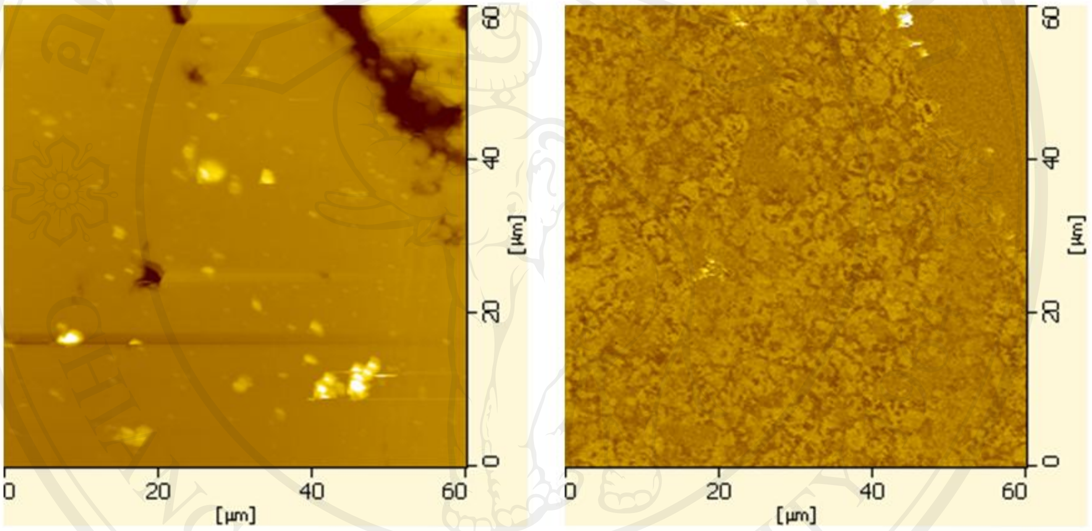

(a) (b)

Fig 4.17 The topography image (a) and the corresponding piezoresponse image (b) for scanning area of 60 x 60μm^2 at interfacial zone of PZT-PC composites

Fig. 4.17(a) and (b) shows the topography and piezoresponse image of 60μm x 60μm scanning areas in interphase between PZT and PC. Grain and Irregular domain patterns are observed in Fig. 4.17(b) and can be clearly seen in the corresponding small scanning areas of 30μmx30μm, 10μmx10μm, as shown in Fig. 4.18 and 4.19, respectively.

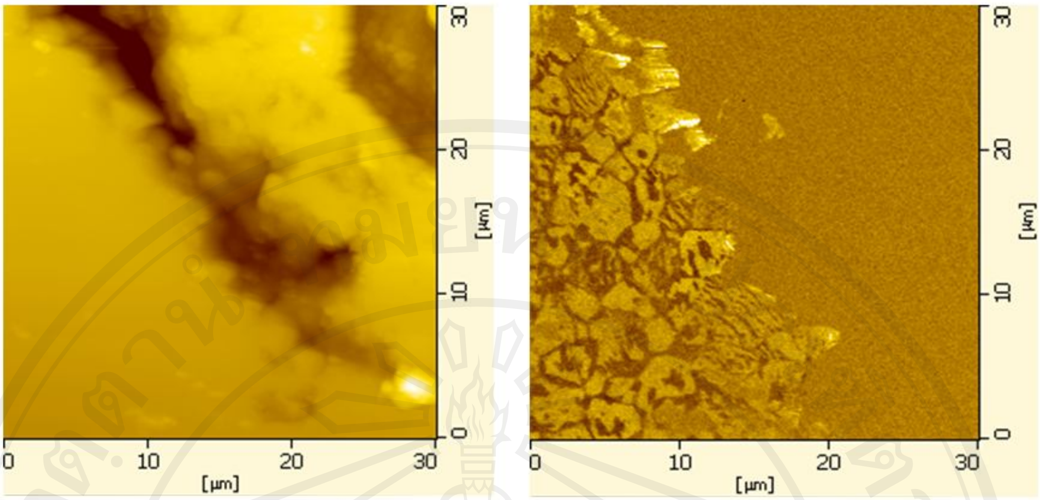

(a) (b)

Fig 4.18 The topography image (a) and the corresponding piezoresponse image (b) for scanning area of 30 x 30μm^2 at interfacial zone of PZT-PC composites

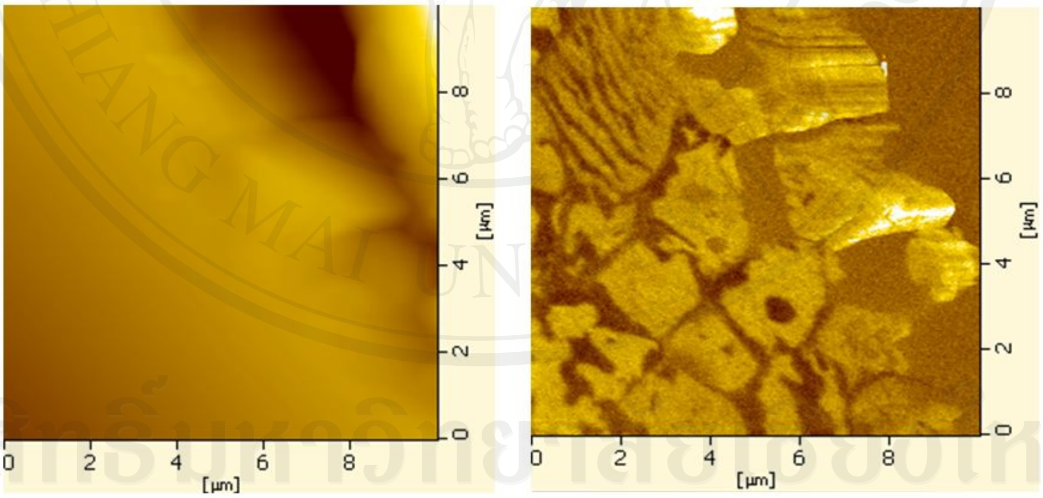

(a) (b)

Fig 4.19 The topography image (a); and the corresponding piezoresponse image (b); for scanning area of 10 x 10μm^2 at interfacial zone of PZT-PC composites

It can be seen that the domain orientated at the interface region in submicron-scale between the piezoelectric phase (PZT) and the Portland cement (PC) phase. However, no piezoresponse from PC phase was found. From topography image of PC phase, a detailed image of the product and pore microstructure was obtained. The pure cement paste has a variable surface intersected by pores, with some part being smooth and some part having a rough surface due to angular particle of cement. The internal surface of the cement paste at the interfacial zone presents small spheroid bulges giving an additional roughness which likely to be that of CSH phase depositing around the pore walls areas [103]. Moreover, in PZT phase the contrast is so strong and the patterns seem to be island like complex structure. In the island like fingerprint pattern, the ferroelectric 180º domain walls have arbitrary orientation [104].

The microstructure of the interface between PZT particles and cement show good bonding which shape of PZT particle, angular aggregate having rough surface appearing to provide better mechanical interlocking with cement paste, however it still found porous at the interfacial zone.

Also, it is interestingly to note that the domain appearance of PZT can be seen to be clearer when PZT were mixed with cement in the composite system than when being investigated on its own under the same magnification as shown in Fig. 4.19 and Fig. 4.16(b) respectively. It is thought that when PZT are mixed with the cement paste and after the paste has set, an internal stress was applied from the cement to PZT as a result of cement hydration subjected to the curing process (60ºC moist cured) thereby giving clearer images of the domain shown inside PZT particles when PZT are produced with cement as composite.

4.6 Summary

Material properties of cement-based piezoelectric ceramic composites are studied both theoretically and experimentally, which include dielectric, piezoelectric, ferroelectric properties and microstructure. The factors, which affect these material properties of composites, are also discussed in detail. The following conclusion can be obtained;

1. 0–3 type cement-based PZT composites can be fabricated using normal mixing and compacting method. It is an easier procedure as compared to those methods for producing PZT/polymer composites.

2. The relative dielectric constant ε_r and piezoelectric strain factor d_{33} obtained from experiment are close to the predictions of the cubes and series model, suggestions that the PZT particles in the composites are uniformly dispersed and closely release to the experiment results. This conclusion is confirmed by SEM images.

3. The d_{33} and ε_r values of the 0–3 cement-based piezoelectric composites show a roughly nonlinear increase as a function of the PZT content. The ε_r experimental values of the composites have a remarkable good agreement with the calculated values.

4. For the 0-3 Portland cement-based piezoelectric composites, the optimum poling conditions are that the poling field E is 2.0kV/mm, the poling time t is 45 min and the poling temperature is 130°C.

5. For the range of particle sizes under 450 μm, the d_{33} increases with increasing particle size of PZT.

6. The 0–3 cement-based piezoelectric composites show typical ferroelectric hysteresis loops at the room temperature. With the increase of the PZT volume fraction, the remnant polarization P_{ir} and the coercive field E_{ic} increase. The remnant polarization displays little asymmetric behavior in the hysteresis loop curves.

7. SEM micrographs show angular piezoelectric ceramic particle bond well with the cement matrix. PFM images show that the domain is orientated at the interface region in submicron-scale between the piezoelectric piezoelectric phase and the Portland cement phase. The amplitude of the piezoresponse signal reflects the local piezoelectricity of the domains in piezoelectric phase where the bright areas in the piezoresponse amplitude image show greater piezoelectricity and the dark areas show weaker piezoelectricity. Moreover, the domain appearance of piezoelectric ceramic can be seen to be clearer when piezoelectric ceramic was mixed with cement in the composite system

Nevertheless, the 0–3 connectivity cement based piezoelectric composites is still difficult to obtain a great piezoelectric properties due to the difficulty in poling ceramic particles in such composite because of the evidence of some pores in a composite. Moreover, in the course of the poling the leakage current is still chiefly caused by the interface pore, the cement matrix pore and their inner water, which has a significant influence on the degree of the poling[15].

The effective ways to improve effectively poling of piezoelectric is to create a continuous electric flux between piezoelectric particles by the introduction of a small volume fraction of a third phase. However, another way to decrease the leakage current caused by the interfacial pores and the cement matrix pores can be implemented by creating a third phase or adding admixture [15] to fill these pores, such as polymer or antifoaming. This was investigated and report in the next part (part II) of this chapter.

PART II

Effect of third phase on microstructure and properties of PZT-PC composites

This second part focuses on improving poling process of ceramic-cement based composite, which PZT ceramic are selected as a piezoelectric phase or disperse phase in the 0-3 system. Then, microstructure and electrical properties such as dielectric, ferroelectric and piezoelectric properties of cement-based piezoelectric ceramic composite is also discussed in details.

For a piezoelectric composite with 0-3 connectivity, the electric field (E_1) acting on the ceramic particles is related to the externally applied electric field (E_0) by [86];

$$E_1 = \frac{3E_0}{2+\frac{\varepsilon_1}{\varepsilon_2}} \tag{4.7}$$

where ε_1 and ε_2 are the dielectric constants of the piezoelectric ceramic and the cement matrix, respectively. Because the dielectric constants of PZT ceramics are much higher than those of cements, the electric field acting on the piezoelectric particles is quite low and insufficient for poling of the ceramics. Therefore, to facilitate the poling of the ceramic particles in the composites, one has to increase the poling field and the poling temperature. Nevertheless, too high a poling voltage can break down the samples and high poling temperature can weaken the mechanical properties of the cement. Alternatively, by adding a small amount of a conductive additive such as carbon graphite, the electrical conductivities of the composite can be adjusted and more continuous electrical flux paths established between ceramic particles. Then the poling process are expected be carried out more easily.

4.7 Dielectric properties

4.7.1 Dielectric properties of PZT-PC composites with added Carbon graphite

Cement based piezoelectric composites used in this investigation were prepared using three raw materials, which are normal Portland cement (PC), lead zirconate titanate (PZT) solid solution was produced by mixed oxide method and carbon graphite powder. Portland cement (ordinary type), PZT ceramic particles of median size of 450 μm and carbon graphite powder were mixed together using PZT volume content 50% and 0, 1, 2 and 5 by volume percentage of carbon graphite powder.

The results shown in Fig. 4.20(a) clearly indicate such a trend that shows the effect of carbon graphite addition on the dielectric properties of PZT-PC composites. The dielectric constants of composite with carbon graphite addition slightly increase with increasing carbon. From the electrical transport (Fig. 4.21), the dielectric properties change dramatically due to formation of a carbon particle percolation path through the composites. According to percolation theory [105], from the electrical transport viewpoint, the carbon graphite /PZT/cement composites can be approximately considered as a two-phase system containing conductive carbon graphite and insulating PZT/cement mixture matrix, which would exhibit a metal-insulator transition with increasing conductive filler concentration. The metal–insulator transition is usually characterized by an abrupt discontinuity in the conductivity and a rapid change in dielectric constant in the neighborhood of the percolation threshold where the conductive particles begin to coalesce into a network [87, 106].

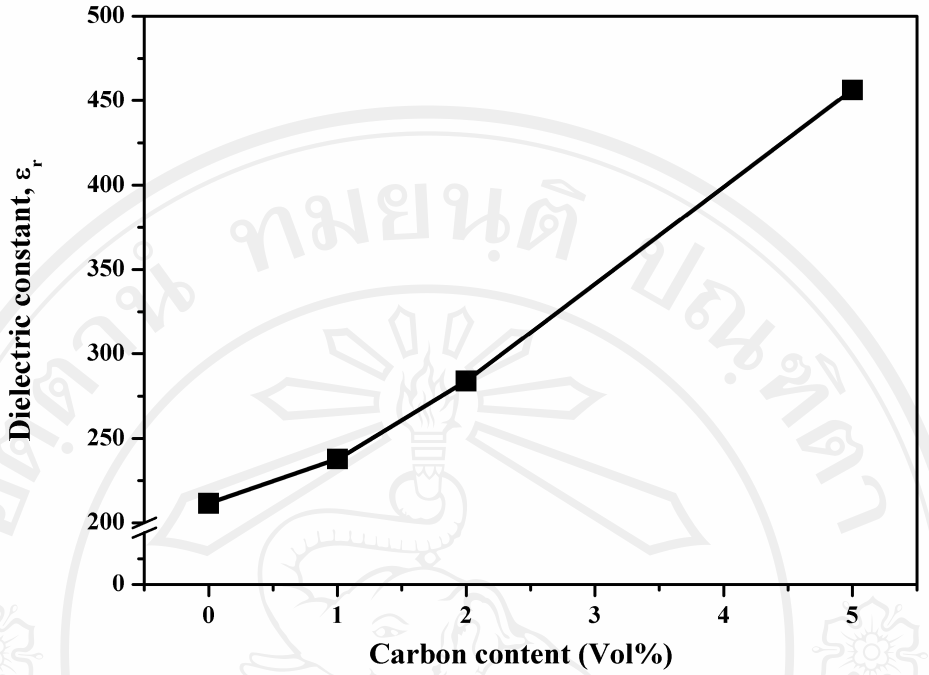

(a)

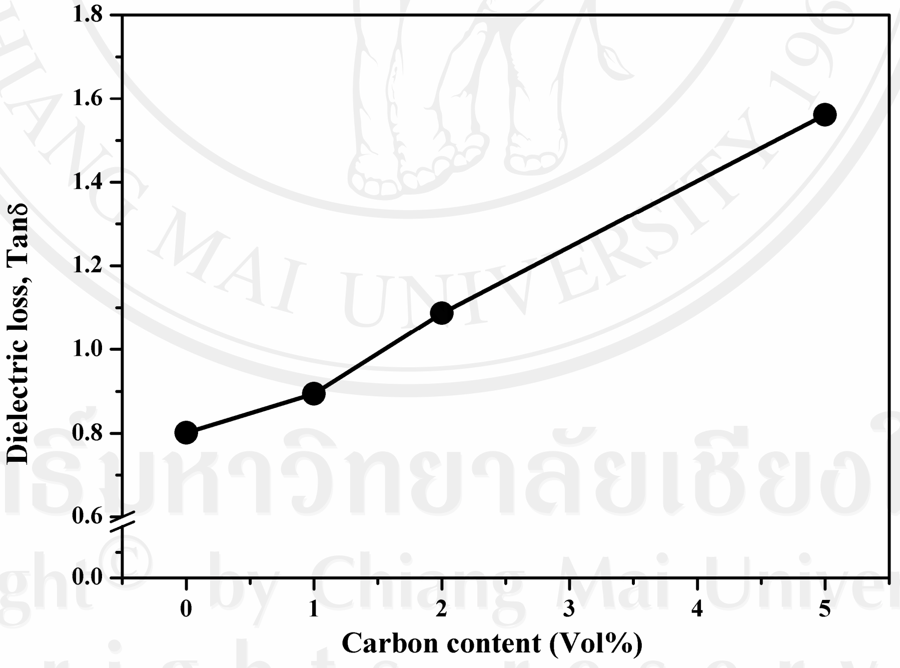

(b)

Fig 4.20 Effect of carbon addition on dielectric properties of PZT-PC composites; (a) dielectric constant; (b) dielectric loss

The dielectric loss, *tan δ* demonstrates a similar feature to the dielectric constant (ε_r) as shown in Fig. 4.20(b). It may be because of the increasing of electrical transport and forming of the conductive network in the composites, there is a sudden jump at around the percolation threshold just as in the case of the dielectric constants. According to the percolation threshold theory, at the threshold value (about 5% in this study), the carbon black particles begin to come into contact in the composite. In this case, the leakage current reaches to its maximum and the composite exhibit very high dielectric loss.

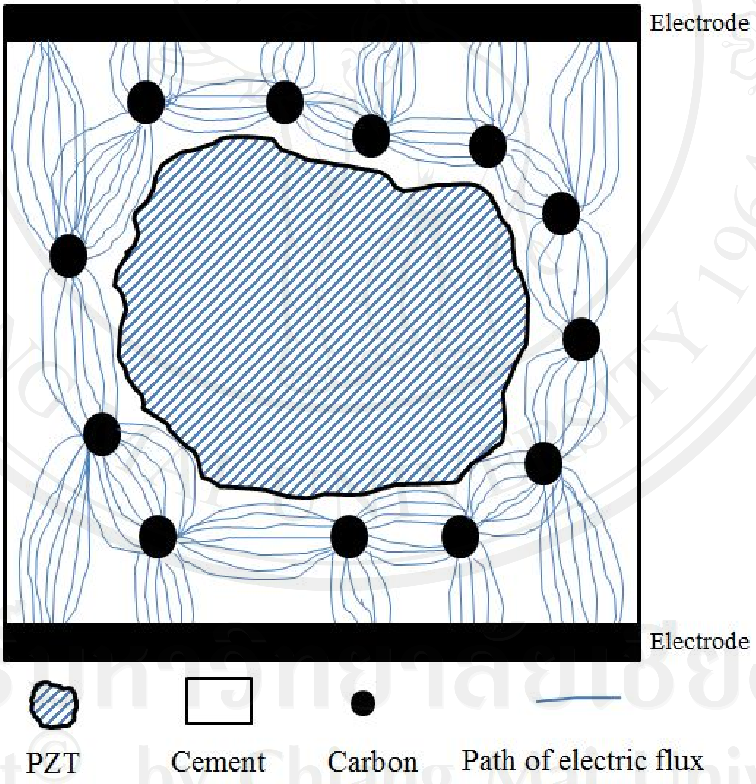

Fig 4.21 Model of electrical transport of PZT-PC composites with added carbon

4.7.2 Dielectric properties of PZT-PC composites with added PVDF

Even though carbon graphite addition can improve the higher dielectric constant, however it also increases the dielectric loss which caused the leakage current in poling process as well. Therefore, a novel approach to effectively improve poling of piezoelectric ceramic is to add an insulator phase between piezoelectric particles by the introduction of a small volume fraction of an insulator phase. In the next part, polyvinylidene fluoride (PVDF) was used as a third-phase with PZT and Portland cement to produce new composites of cement-PZT-PVDF combination. The dielectric properties and piezoelectric properties (d_{33} and g_{33}) include poling period of the composites were then investigated.

Portland cement, PZT ceramic and PVDF were mixed together and axially pressed into disks of 15 mm in diameter and ≈ 2 mm in thickness to form PZT-PVDF-PC composites using PZT volume content 50% and 1, 2 5, 10 and 20% volume of PVDF content.

The dielectric constant of PZT-PVDF-PC composites is shown in Fig. 4.22(a). The dielectric permittivity of the composites slightly increases with increasing the contents of PVDF to 2%Vol; after that the ε_r was found to decrease almost linearly when adding the PVDF up to 10%Vol. Moreover, it can be seen from Fig. 4.22(b) that the dielectric loss decreases almost linearly with increasing PVDF content. In this consideration, it is expected that the PVDF addition can improve the piezoelectric properties. The next section reports the use of third phase addition (PVDF) in PZT-PC composite on the piezoelectric properties and the poling period.

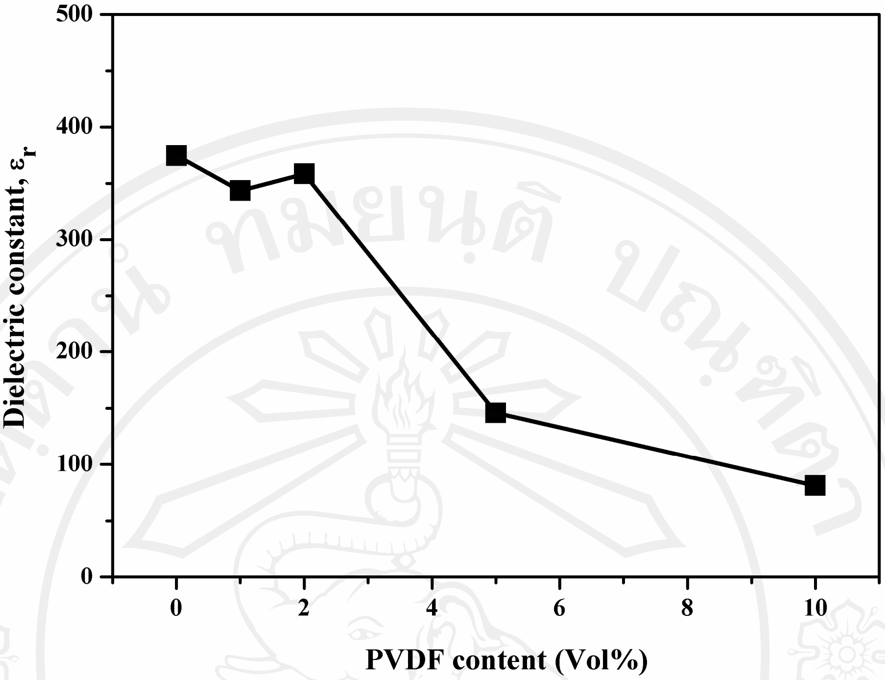

(a)

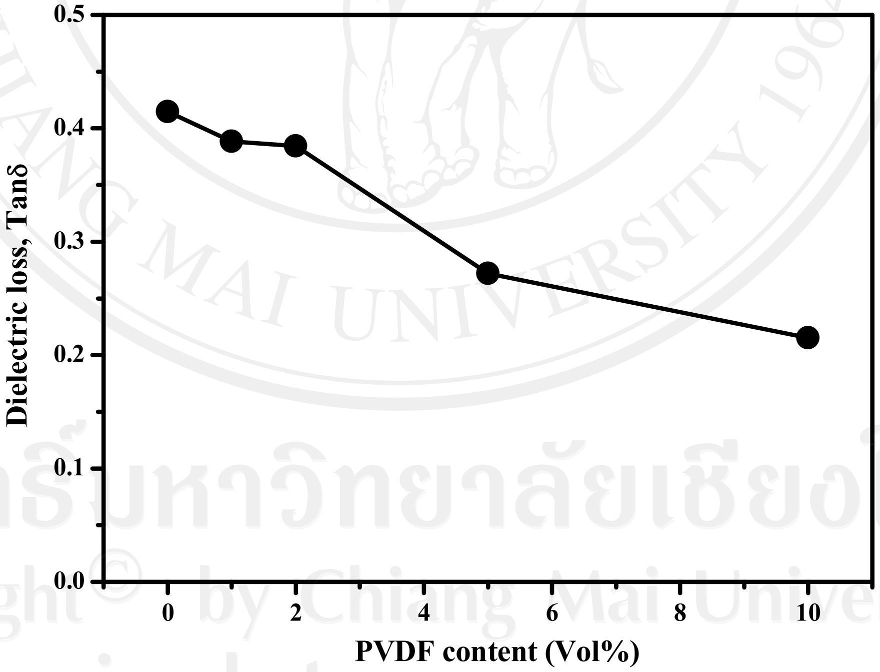

(b)

Fig 4.22 Effect of PVDF addition on dielectric properties of PZT-PC composites; (a) dielectric constant; (b) dielectric loss

4.8 Piezoelectric properties

4.8.1 Piezoelectric properties of PZT-PC composites with added Carbon graphite

In this part the effect of carbon graphite and PVDF addition on both piezoelectric properties as d_{33} and g_{33} were investigated under the optimum poling condition of poling field at 1kV/mm, poling temperature as 130°C, and poling time at 45 min, respectively. From the results in Fig. 4.23, it can be seen that the d_{33} values increase with carbon graphite addition with 1% Carbon graphite. However, when the added carbon exceeds 1 vol.%, it found that high energy loss at this poling stage makes it difficult to apply the voltage required for poling PZT particles because the electric energy is dissipated by large leakage current and could lead to a higher chance for break down of sample.

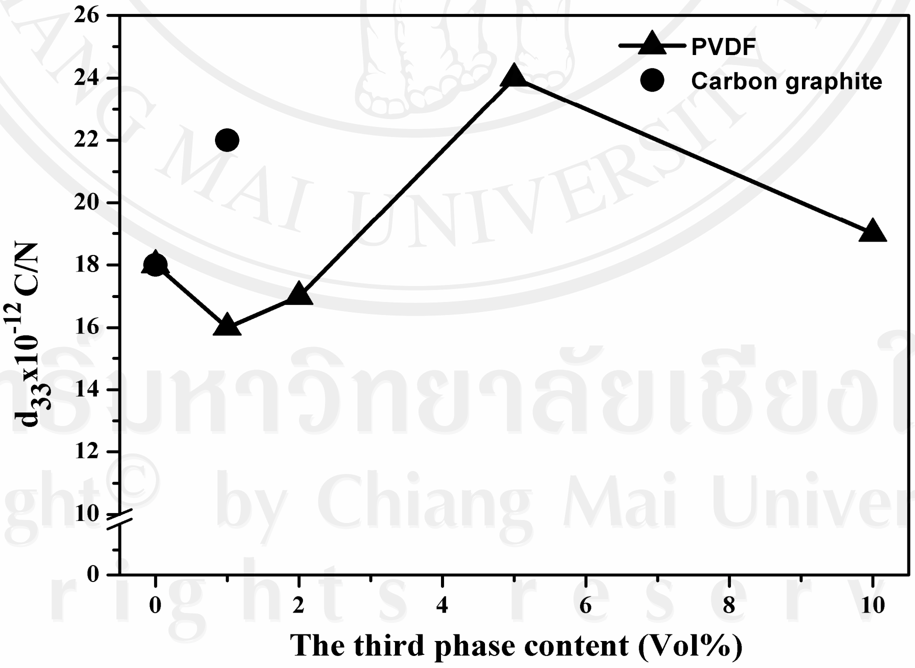

Fig 4.23 The piezoelectric charge coefficient (d_{33}) of PC-PZT composites with various PVDF and carbon graphite additions

4.8.2 Piezoelectric properties of PZT-PC composites with added PVDF

Meanwhile, the variation of piezoelectric coefficient as a function of the content of PVDF and carbon graphite has been studied and the results are also shown in Fig. 4.23. It can be seen that a significantly nonlinear change of the d_{33} values of the composites were found as a function of the PVDF content. Initially there is a small decrease, but when the content of PVDF exceeds 2%, the d_{33} values increase much more sharply. Then, the d_{33} values decrease when the PVDF content more than 5%Vol.

From these results, it can be explained in term of PVDF addition that, the initially d_{33} values (with 0, 1 and 2%PVDF) do not change significantly. At low concentration PVDF, the insulator from small clusters of nearest neighbor sites and they are not connected by a path of nearest-neighbor insulator sites [107], so a current cannot flow between them. Whereas, the pore sites between clusters of CSH phase (hydration product of cement) represent conductor, and that electrical current can only flow between them and leading to the leakage current. At 5% PVDF addition the d_{33} value is highest which can be explained from the fact that at more PVDF concentration, the mixture is acting as an insulator, with less conducting path connecting the porosity or conducting ion in the system, resulting to greater electrical current flowing to PZT phase. At some concentration in between, therefore, a threshold concentration must exist where for the first time electrical current can percolate from one edge to the other or where the system change from a conductor to an insulator. The threshold concentration is called the percolation threshold or the critical concentration, since it separates two different phases [107].

In order to compare the poling period between PVDF and carbon graphite, it is also verified from Fig. 4.24 that with the increase in PVDF content. There is a nearly linear decrease in the poling period whereas when compound to the carbon graphite addition (section 4.8.1), there is an increase in the poling period.

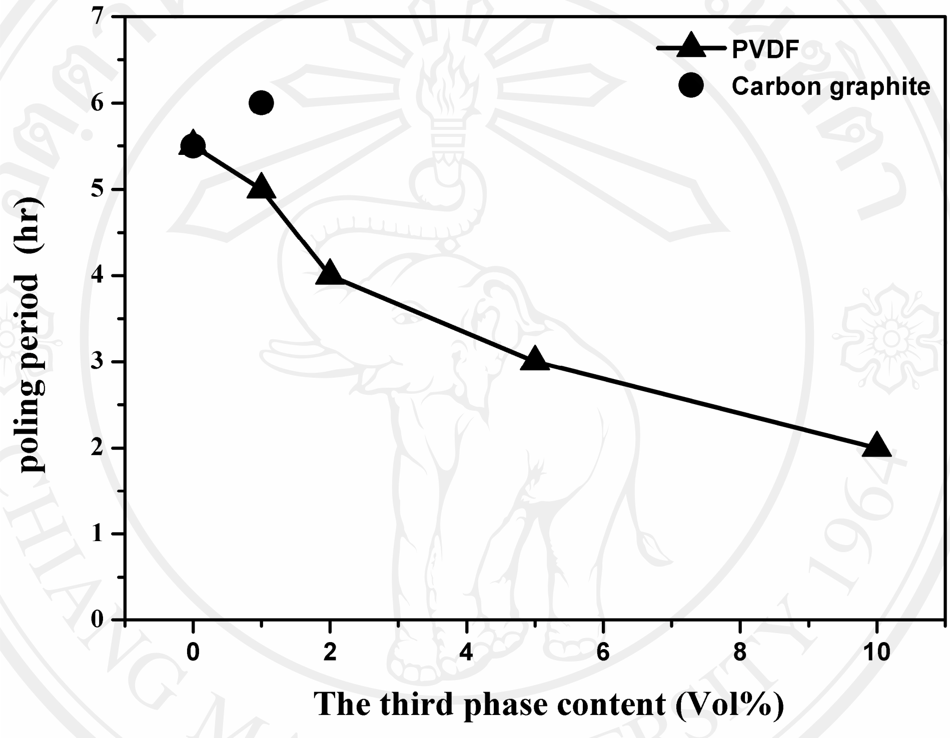

Fig 4.24 The poling period of PZT-PC composites with various PVDF and carbon graphite additions

Therefore, an analysis of the results in Fig. 4.24 may confirm the validity of these hypotheses that the PVDF addition is much more efficient than carbon graphite addition in improving the poling process thus reduce the poling period. The results between PVDF and carbon graphite in term of the dielectric permittivity, ε_{33} and the piezoelectric voltage coefficient, g_{33} can be seen in Figs. 4.25 and 4.26 respectively.

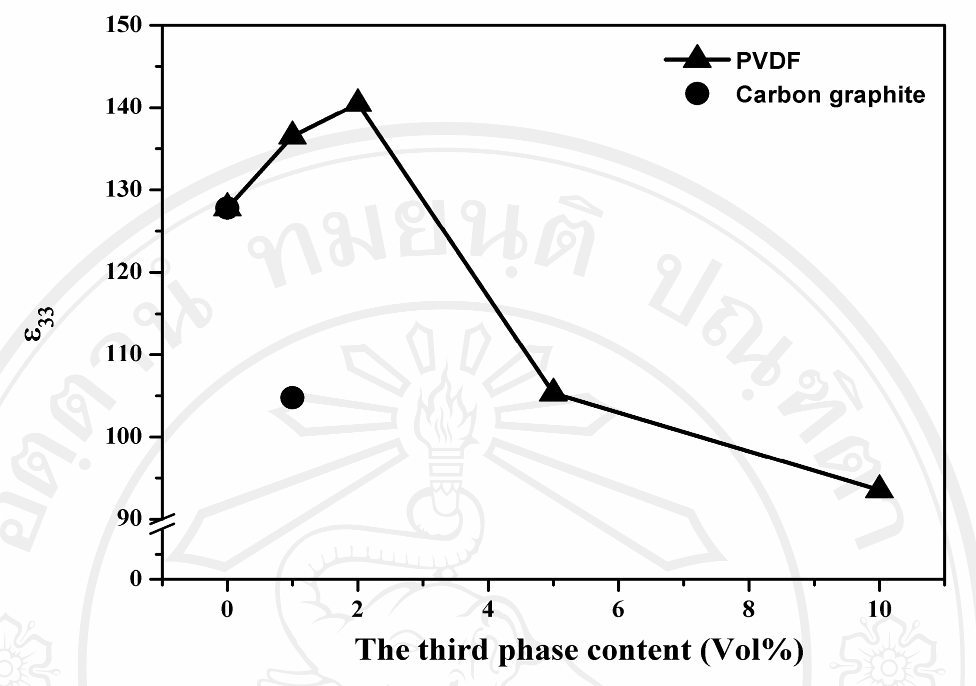

Fig 4.25 The dielectric permittivity (ε_{33}) of PZT-PC composites with various PVDF and carbon graphite additions

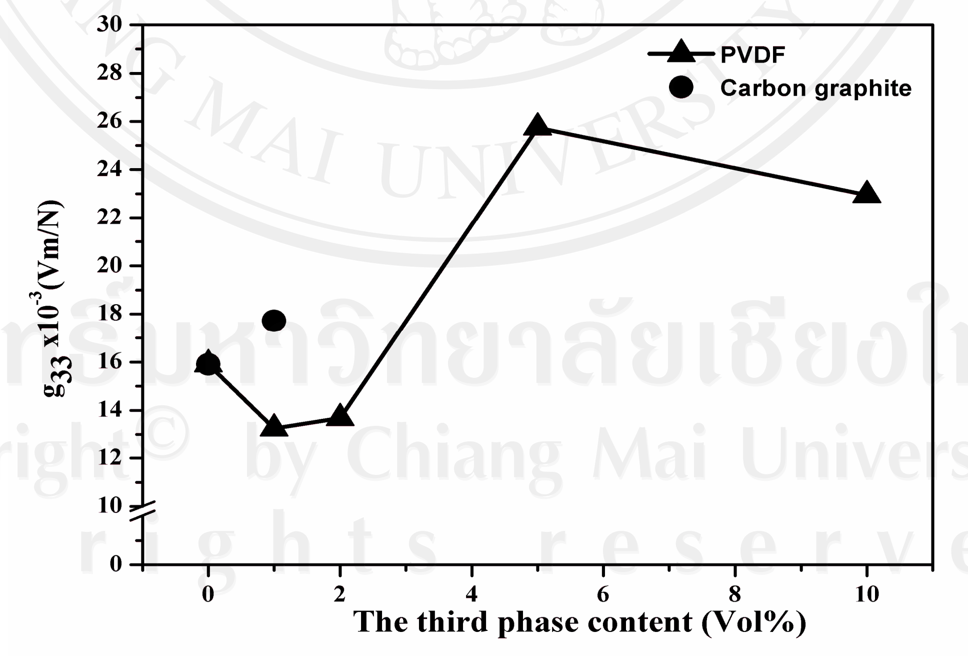

Fig 4.26 The piezoelectric voltage coefficient (g_{33}) of PZT-PC composites with various PVDF and carbon graphite additions

The dielectric permittivity (ε_{33}) after of the composites slightly increases with increasing the contents of PVDF to 2%Vol., after that the ε_{33} was found to decrease almost linearly when adding the PVDF up to 10%Vol. whereas the ε_{33} steady decreases with increasing carbon graphite content up to 1%Vol. due to the longer poling period.

The effect of the piezoelectric voltage factor, g_{33}, on the PVDF content is shown in Fig. 4.26. It can be seen that the g_{33} results have similar trend to that of d_{33} values, where at 5% PVDF addition the g_{33} showed highest value of 25.7 x10^3 Vm/N. Moreover, when the PVDF content was used at higher than over 5% by vol, g_{33} decreases slowly. The main reason is that upon increasing the PVDF content, the dielectric permittivity of the composites with higher vol% of PVDF (10 % PVDF) after poling are higher than that of the composite at 5% PVDF addition, since g_{33} is calculated as $g_{33} = d_{33}/\varepsilon_0\varepsilon_{33}$.

In addition, it can also be observed from Fig. 4.24 that if the PVDF content continuously increases, poling period will be reduced. This is may be due to the absence of some matrix pores, as a result of adding more PVDF in the composite. Nevertheless, the piezoelectric properties (d_{33} and g_{33}) directly depend on the poling conditions of the composites. In general, the poling electric field, the poling temperature and the poling time, all has an effect on the piezoelectric properties of the composites. The poling conditions are often confined by some factors, such as character of each component phase of the composites, defects formed during preparation and especially the microstructure [15, 85].

4.8.3 Effect of hydration ages on piezoelectric properties

The variation of piezoelectric coefficient, d_{33}, of various PVDF/PZT/cement composites as a function of aging time is shown in Fig. 4.27. The samples were all polarized under a DC electric field of 1 kV/mm for 45 min at 130°C. It can be seen that the piezoelectric coefficients of the composites were sensitive to PVDF (1-10%Vol) addition. At the PVDF contents of 5.0-10.0 vol.%, the d_{33} increase slowly in the first 5 days after poling and then become almost stable over the next 30 days. For the addition of PVDF 1.0-2.0%Vol, during the first 5 days after poling the d_{33} increases steadily and then increase more slowly the next 30 days. The variation of piezoelectric voltage factor (g_{33}) with various PVDF phase/PZT/cement composites as a function of aging time is also plotted in Fig. 4.28. The g_{33} values were calculated using the measured values of d_{33} coefficients and the dielectric constants of the composites (Fig 4.29).

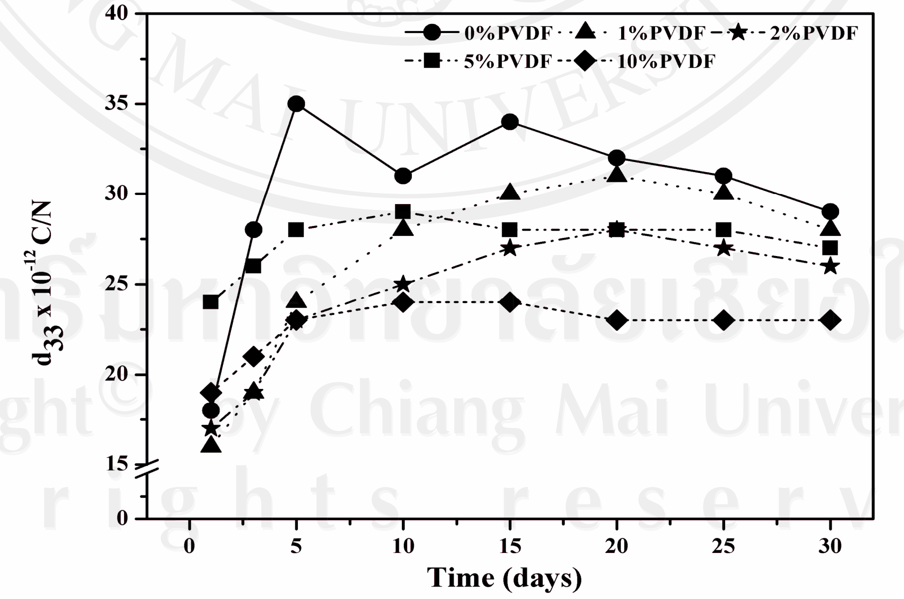

Fig 4.27 The effect of hydration age on the piezoelectric charge coefficient (d_{33}) of composite for 30 days of PVDF addition

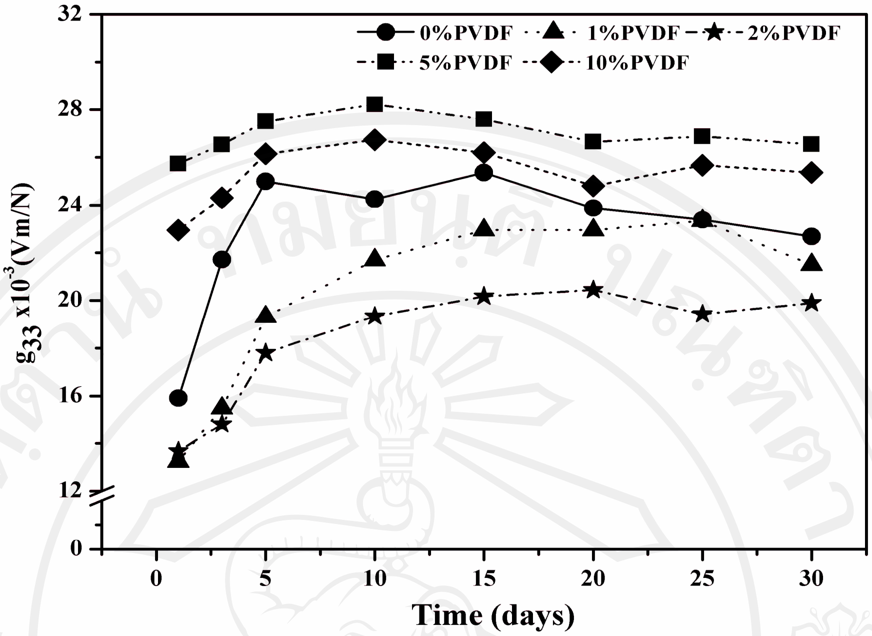

Fig 4.28 The effect of hydration age on the piezoelectric voltage coefficient (g_{33}) of composite for 30 days of PVDF addition

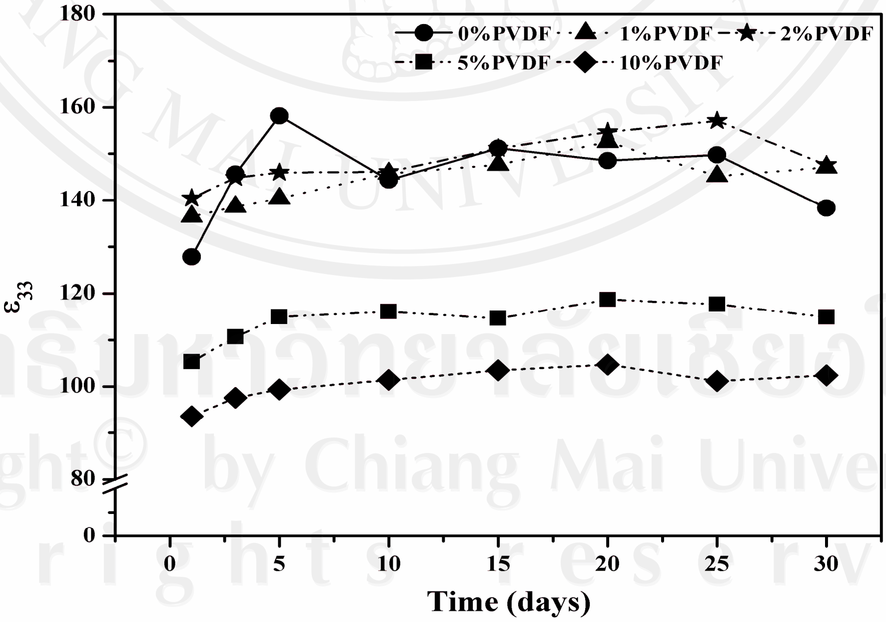

Fig 4.29 The effect of hydration age on the dielectric permittivity (ε_{33}) of composite for 30 days of PVDF addition

The composites containing PVDF from 5.0 to 10.0 vol% show high g_{33} values. This is a consequence of the more rapid increase in d_{33} than that in ε_{33}. The very low g_{33} for the composite with 1.0-2.0 vol% is due to the relatively low d_{33} coefficient and high dielectric constant compared to the composites containing PVDF from 5.0 to 10.0 vol%. From these results, the d_{33} values of the composites increased slowly and approached a relatively steady state after 10 day.

Aging is mainly relate to the rearrangement of ferroelectric domains and an intrinsic property of piezoelectric ceramics. The 90° and 180° ferroelectric domains of piezoelectric ceramics are forced to rotate so as to be parallel to the direction of the electric field under an externally applied high voltage. The orientation of the 90° domains will generate great internal stress on domain walls, which in turn means excites the material to a high-energy non-equilibrium state. The 90° domains have a tendency to revert to random states to release the residual internal stresses when the poling field is removed, after which the piezoelectric properties degrade gradually with time [108].

However, the piezoelectric ceramic cement-based composites exhibit a very different aging behavior from the piezoelectric ceramics. As demonstrated in Fig. 4.25 and 4.26, there is no reduction of d_{33} and g_{33}. On the contrary, an increase of d_{33} and g_{33} values on the 30 days was observed. The slight increase of d_{33} value of cement-based ceramic piezoelectric composite with aging has been reported by Li *et al.* and Cheng *et al.* [78, 85] they believed it might be due to the increase of interfacial stresses between cement and ceramic particles as cement undergoing hydration process. PVDF has an effect on the aging of the composites with the addition of 1.0–10.0 vol.% PVDF the d_{33} and g_{33} value showed a remarkable increase but considerable fluctuations for several days after poling. However, the main component as cement matrix has a strong effect on the aging more than a third phase as PVDF. On one hand, the significant increase of d_{33} and g_{33} values indicates that more ferroelectric domains of the piezoelectric ceramic fillers were orientated. On the other hand, the fluctuation of d_{33} and g_{33} values is supposed to be related to the structural characteristics of cement.

4.9 Ferroelectric properties

In this part, composites consisting of PC matrix and PZT ceramic, with various carbon graphite and PVDF addition, were prepared using the pressed and cured method in which the samples were first pressed together before curing. The PZT ceramic particles were then mixed with PC to produce 0–3 connectivity using 1:1 PZT ratio by volume. Carbon graphite and PVDF was also added as the third phase in the composite at 0, 1 and 2% by volume of carbon graphite and at 0, 1, 2, 5 and 10% by volume of PVDF. Ferroelectric hysteresis (*P*-*E*) loops were determined at room temperature and an electric field at 20kV was applied to a sample with an input sinusoidal signal and a frequency of 50 Hz.

4.9.1 Ferroelectric properties of PZT-PC composites with added Carbon graphite

The hysteresis loops at various carbon graphite is shown in Fig. 4.30. From Fig. 4.30, it should be noted that a lossy behavior can be seen to be more sensitive at higher carbon graphite especially at 2% by volume where an oval shaped typical of conduction is seen.

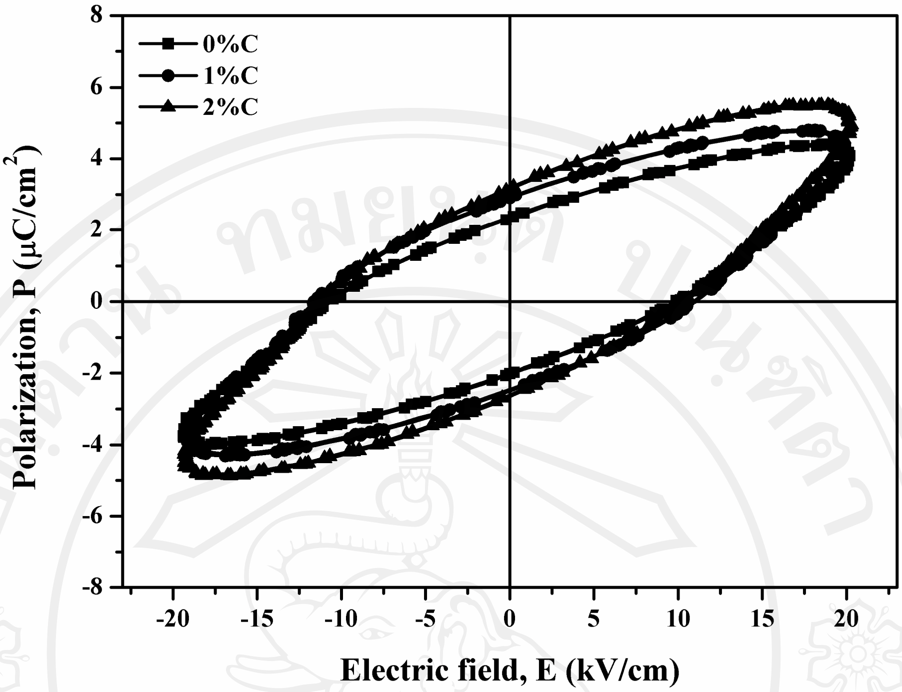

Fig 4.30 Effects of carbon graphite content on the ferroelectric (*P-E*) hysteresis loops of PZT-PC composites (with fixed *f* of 50 Hz) of external electric field amplitude at 20kV/cm

At high carbon graphite content, when an external electrical field (20kV) acts on the cement matrix many weak conducting ions such as Ca^{2+}, OH^-, Al^{3+} from cement matrix and conducting phase as carbon graphite begin to migrate besides the dipolar activity. These ions cause higher conducting loss in the composites.

4.9.2 Ferroelectric properties of PZT-PC composites with added PVDF

The polarization-electric field (P-E) loops of PZT ceramic–Portland cement composites, with added PVDF, are shown in Fig. 4.31. It should be noted that all ferroelectric hysteresis loops (*P-E* loops) of the PZT ceramic-cement composites also show a small lossy feature, with round tips as a result of cement matrix in the composites. It is clear from these hysteresis measurements, that the PVDF phase has an effect on the polarization-electric field loop, where composites with added PVDF phase are found to show higher polarization with lower loss.

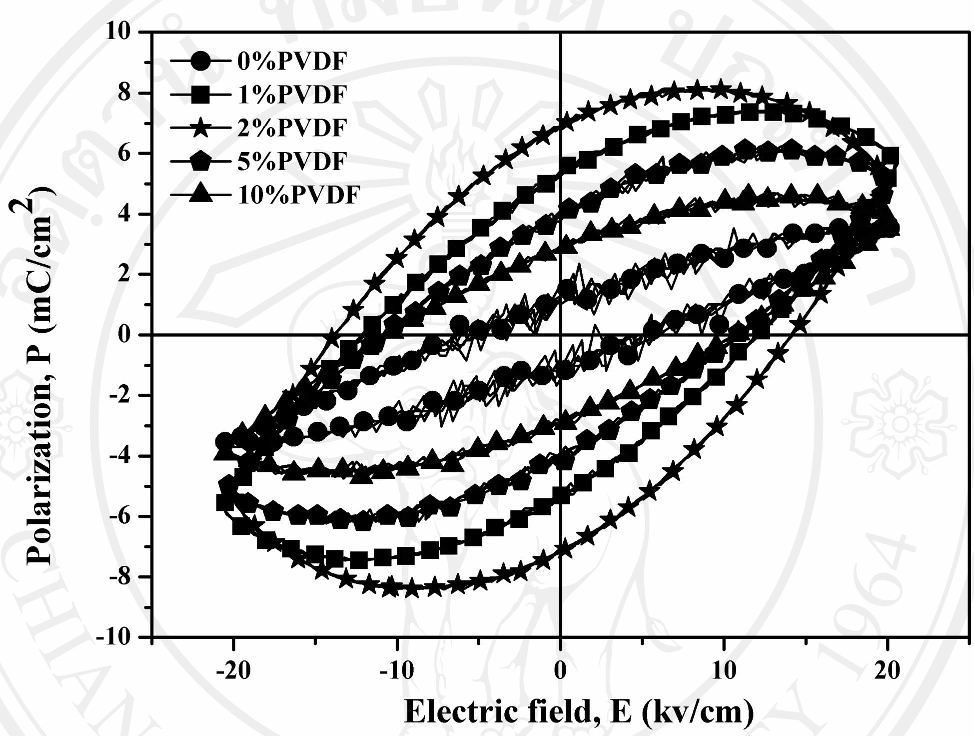

Fig 4.31 Effects of PVDF content on the ferroelectric (*P-E*) hysteresis loops of PZT-PC composites (with fixed *f* of 50 Hz) of external electric field amplitude at 20kV/cm

When using PVDF as the third phase at 2% by volume, the P_{ir} value was found to be highest. The PVDF phase thereby acts as a insulating phase in cement matrix and also as a connecting network phase takes the place of porosity between the cement matrix and PZT ceramic particles. Therefore, this would suggest, that adding the PVDF phase to the composite system, would decrease the conducting ion within the cement matrix and giving better piezoelectric properties.

4.10 Interfacial morphology and Microstructure

4.10.1 Microstructure of PZT-PC composites with added PVDF

From previous investigation, it is reasonable to assume that in the course of the poling the leakage current is still chiefly caused by the interface pore, the cement matrix pore and their inner water, which has a significant influence on the degree of the poling, the effective ways to effectively improve poling of piezoelectric ceramic is to add insulator phase as PVDF between piezoelectric particles by the introduction of a small volume fraction of a third phase.

Therefore, in this part, Scanning electron microscope and high resolution piezoresponse force microscope were used to investigate the interfacial region and pore-filled polyvinylidene fluoride (PVDF) addition on PZT piezoelectric ceramic-Portland cement based composites. PZT ceramic particles of median size of 450 μm were used in this study. Then, Portland cement, PZT ceramic and PVDF were mixed together and axially pressed into disks of 15 mm in diameter and about 1.75 mm in thickness to form PZT-PVDF-PC composite using PZT volume content 50% and 5 by volume percentage of PVDF. Afterwards, PZT–PVDF-PC pellet composites were kept in curing chamber with 97% RH at 60 ºC for 3 days before measurement.

The SEM images and the EDX spectrums of the povinylidene fluoride (PVDF) are shown in Fig. 4.32 (a-c and d) where povinylidene fluoride (PVDF) powders can be seen to be in the region of ~0.2 μm in diameter size and also be seen to be spherical in shape. The EDX spectrums (Fig 4.32 (d)) shows weight% of main element of PVDF is Carbon; C as 45.91, Oxygen; O as 2.82 and Fluorine; F as 51.27, respectively.

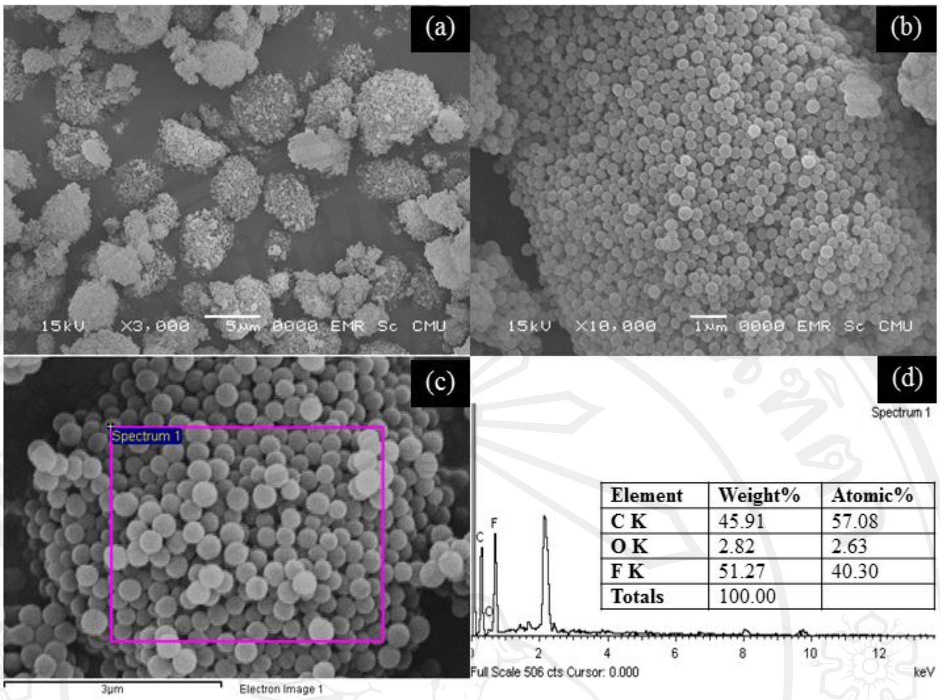

Element	Weight%	Atomic%
C K	45.91	57.08
O K	2.82	2.63
F K	51.27	40.30
Totals	100.00	

Fig 4.32 SEM micrographs of PVDF powder (a) magnification ×3,000, (b) magnification ×10,000, (c) magnification ×20,000 and (d) EDX spectrum

PFM topography mode images of the povinylidene fluoride (PVDF) are shown in Fig. 4.33(a, b and c) which represents the scanning areas of 70μm x70 μm, 30μm x30 μm and 10μm x10 μm, respectively. The topography image shows the microstructure of the surface, scanned in a humid air environment at room temperature in which the image voltage has amplitude of 12 V and a frequency of 8 kHz. Fig 4.33 (a) and (b) shows the spherulitic structure of the neat PVDF and interface between spherulites at an isothermal crystallization temperature of 160°C of semicrystalline α-type PVDF [109] (below the melting temperature T_m at 178 °C, PVDF crystallizes from the homogeneous melt [110, 111]. The spherulites are observed in form of radial lamellar splay pattern which dependence of band periodicity on crystallization temperature [109] as shown in Fig 4.33 (c).

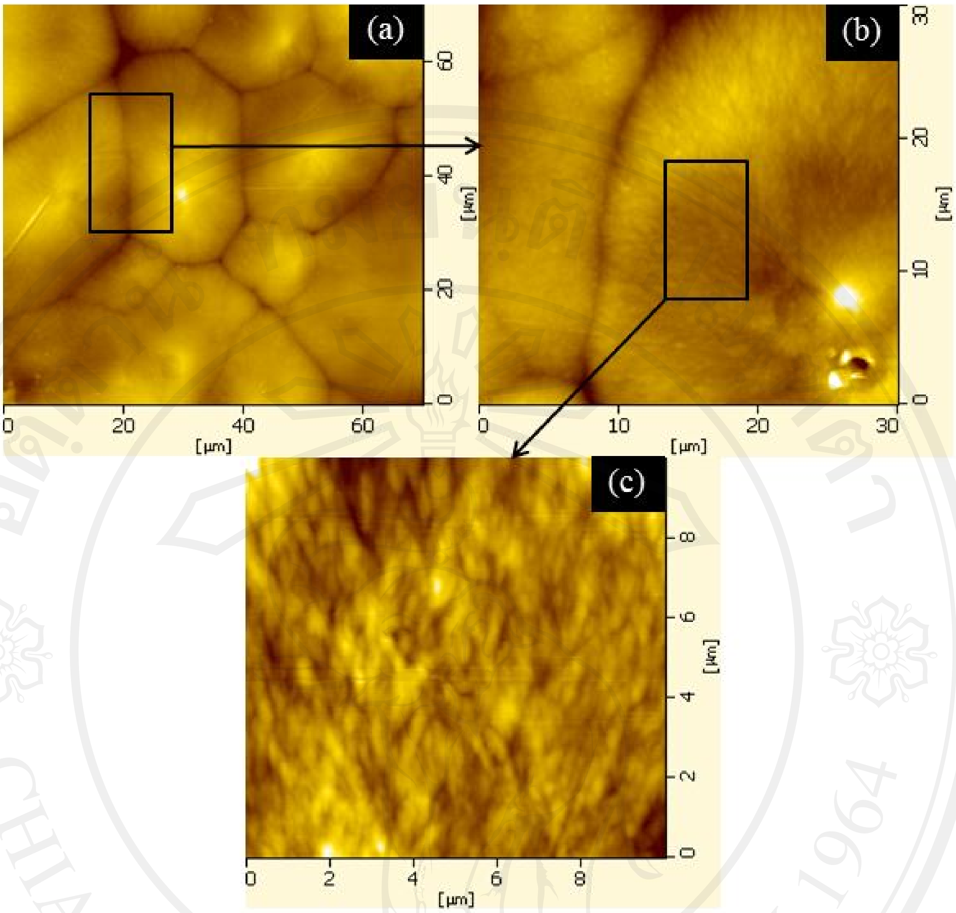

Fig 4.33 The topography image for scanning area of (a) 70 x 70μm^2, (b) 30 x 30μm^2, (c) 10 x 10μm^2 of PVDF

Fig. 4.34(a) and (b) shows the topography and piezoresponse image of 30μm x 30μm scanning areas in interphase between PZT and PC. In addition, many pores are intersected in a variable interphase and between clusters of CSH phase [102]. Moreover, The cement phase at the interfacial zone presents small spheroid bulges giving an additional roughness which likely to be that of CSH phase depositing around the pore walls areas [112].

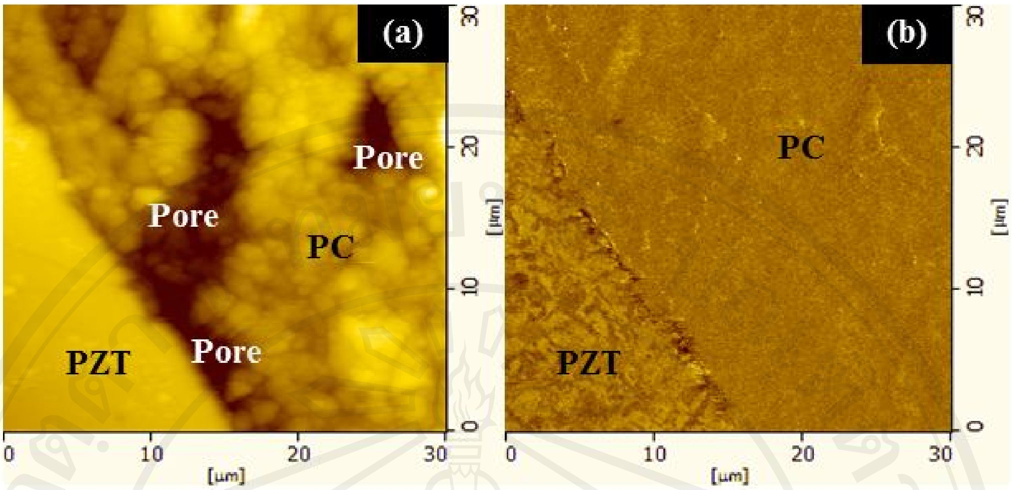

Fig 4.34 The topography image (a) and the corresponding piezoresponse image (b) for scanning area of 30 x 30μm^2 at interfacial zone of PZT-PC composites

Furthermore, it can be clearly seen in the corresponding small scanning areas of 10umx10um, as shown in Fig. 4.35(a) topography image and (b) piezoresponse image, respectively. From Fig 4.35(c), a detailed image of pore microstructure was obtained and showed pore size in submicron-scale ~1.28 μm, approximately. However, no piezoresponse from PC phase was found in Fig 4.35(b) whereas in PZT phase where the bright areas in the piezoresponse amplitude image show greater piezoelectricity and the dark areas show weaker piezoelectricity [91, 92]. The amplitude and phase of the piezoresponse signal are related to the magnitude of the piezoelectric coefficient and the direction of local polarization, respectively. The irregular bright and dark contrasts regions in PZT phase are found to be antiparallel polarization domains, i.e. 180° domains [113, 114]. Moreover, the domain appearance of PZT can be seen to be clearer when PZT was mixed with cement in the composite system.

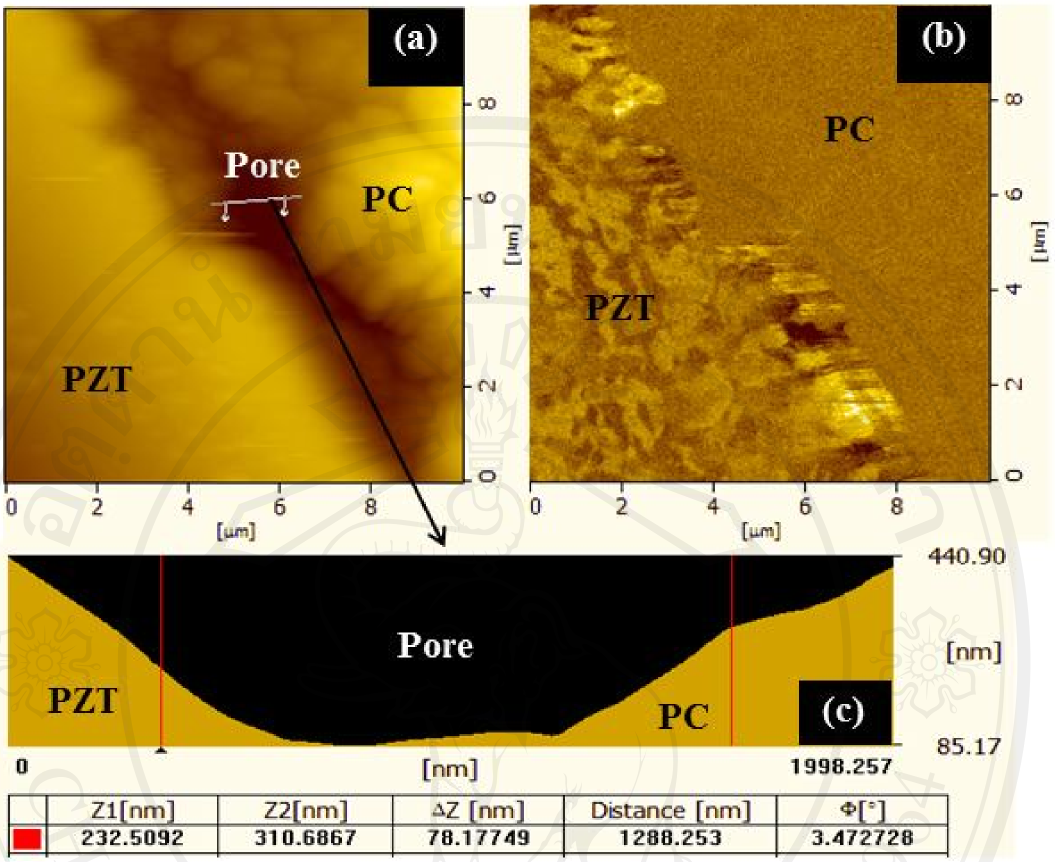

	Z1[nm]	Z2[nm]	ΔZ [nm]	Distance [nm]	Φ[°]
🟥	232.5092	310.6867	78.17749	1288.253	3.472728

Fig 4.35 The topography image (a); the corresponding piezoresponse image (b) and pore size (c) for scanning area of 10 x 10μm^2 at interfacial zone of PZT-PC composites

Fig 4.36 (a-c and d) shows the SEM micrograph and the EDX spectrums of the PZT-PVDF-PC composites. From Fig 4.36(a-c), a relatively dense matrix of PVDF and cement can be seen surrounding that of PZT particle and PVDF show good binding by filling the pores fully at the interface region between PZT phase and the Portland cement phase. The EDX spectrums (Fig 4.36(d)) of the materials filling in the pore to be that of PVDF showing weight% of element of PVDF and cement.

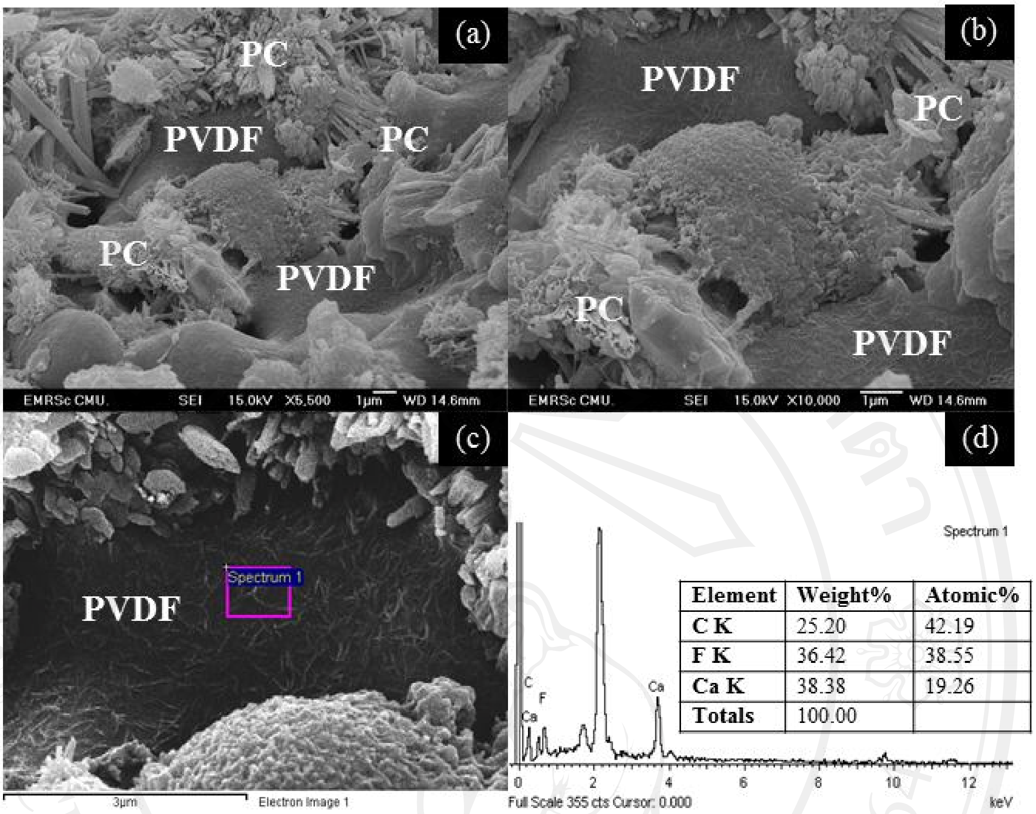

Element	Weight%	Atomic%
C K	25.20	42.19
F K	36.42	38.55
Ca K	38.38	19.26
Totals	100.00	

Fig 4.36 SEM micrographs of PZT-PVDF-PC composites (a) magnification ×5,500, (b) magnification ×10,000, (c) magnification ×20,000 and (d) EDX spectrum

Fig. 4.37(a-c) shows the topography image in the interphase between PZT and PC with PVDF. The scanning areas among PZT, PC and PVDF are 30μm x30μm (Fig 4.37 (a)) and it can be clearly seen in the corresponding small scanning areas of 10μm x 10μm, as shown in Fig 4.37 (b and c) in which amplitude of 12 V and a frequency of 8 kHz. The microstructure of the interface between PZT particles and cement show good bonding of PZT particle and it is believed to contribute to better mechanical interlocking with the cement paste [101, 115] with porosity are filled by PVDF as a binder at the interfacial zone. In addition, the piezoresponse image in the interphase region between PZT and PC with PVDF as a binder can be clearly seen in Fig 4.38(a-c). The piezoresponse image shows that in PZT phase, the contrast is so strong and the patterns seem to be island like complex structure. In the island like fingerprint pattern, the ferroelectric 180º domain walls have arbitrary orientation [116]. Moreover, the piezoresponse image shows structure of the neat PVDF in form of lamellar splay pattern at the interphase of PZT and PC. However, no piezoresponse from PC phase was found.

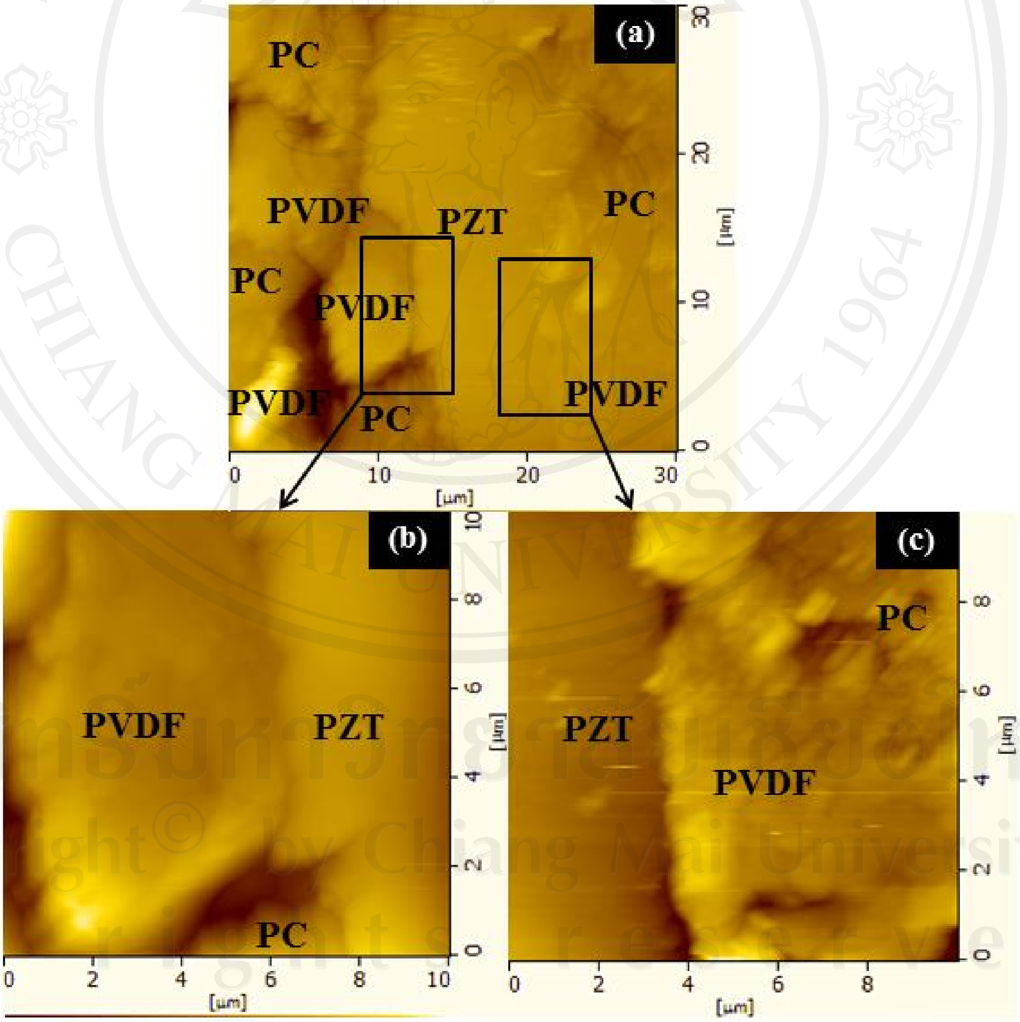

Fig 4.37 The topography image for scanning area of 30 x 30μm^2 (a), 10 x 10μm^2 (b and c) of PZT-PVDF-PC composite

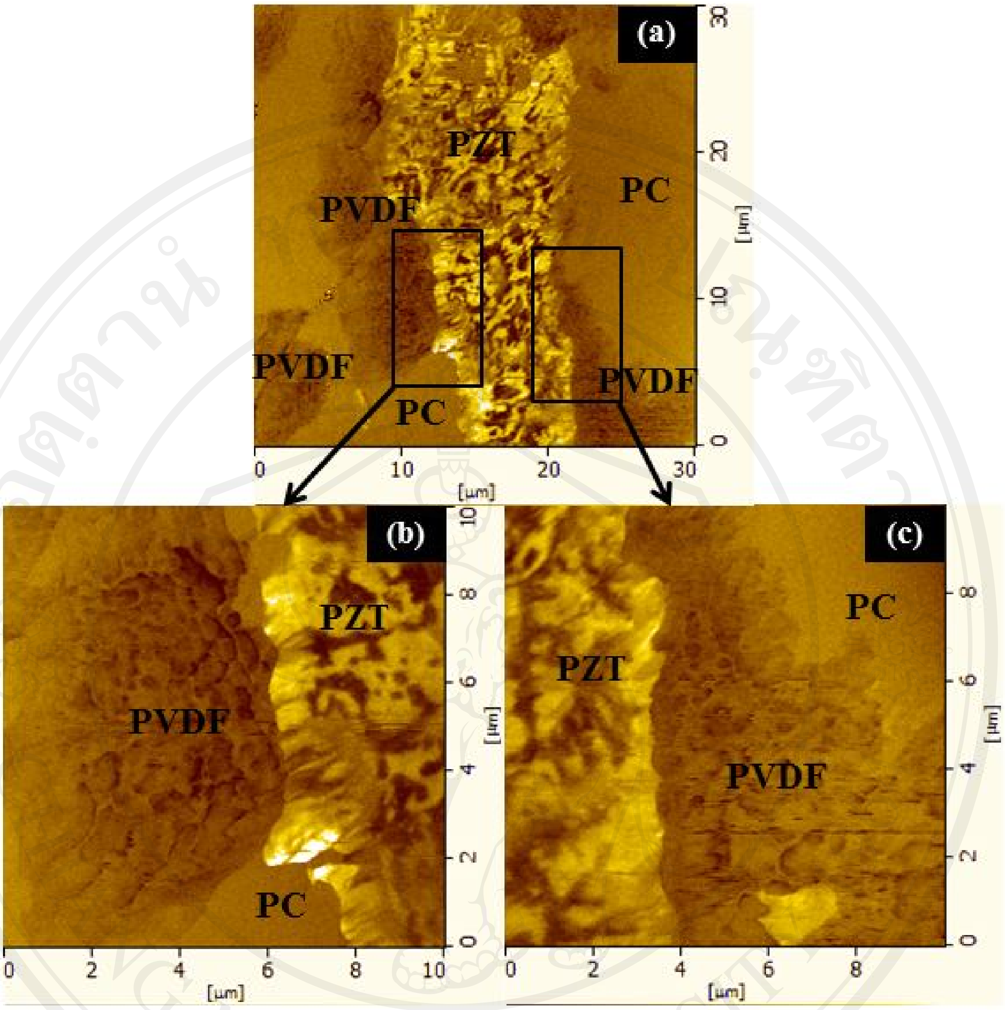

Fig 4.38 The corresponding piezoresponse image for scanning area of 30 x 30μm^2 (a), 10 x 10μm^2 (b and c) of PZT-PVDF-PC composite

4.11 Summary

In this chapter, microstructure and electrical properties of cement-based PZT ceramic composites with third phase addition are studied, which include dielectric, piezoelectric, ferroelectric properties and microstructure include phase and interface. The factors, which affect these material properties of composites, are also discussed in detail. The following conclusion can be obtained;

1. PZT-C-PC composite (when ratio of PZT to PC were 50 volume percentages and carbon was 1.0 to 10.0 percentage of volume) were prepared from PZT ceramic carbon and PC powders. The dielectric properties of the composite were determined at room temperature and frequency between 1 kHz. The results indicate that the dielectric properties of the pure phase PZT and PZT-C-PC composites follow that of normal ferroelectric behaviors. Both dielectric constant and loss of composite with carbon addition increase with increasing carbon.

2. Cement based-PZT-PVDF composite were prepared from PZT ceramic PVDF and PC powders using PZT volume content 50% and 1, 2, 5 and 10% volume of PVDF content. The piezoelectric charged coefficient (d_{33}) and piezoelectric voltage coefficient (g_{33}) were found to increase with the addition of PVDF especially when used at 5% PVDF addition where d_{33} is 24 pC/N and g_{33} is 25.7 x10^3 Vm/N respectively. Also, the PVDF addition in the composite can solve the problem relating to the poling process of these composite resulting significantly less poling time being used.

3. Ferroelectric hysteresis loop showed an increase in the polarization in PZT-Portland cement composites when PVDF is added as the third phase. Therefore, this would suggest, that adding the PVDF phase to the composite system, would improve

the network within the cement matrix (the three-dimensional matrix) and that poling can be enhanced, giving better piezoelectric properties.

4. PFM images show PZT ceramic particles bond well with the cement matrix with mechanical interlocking while PVDF show good connection by the pore filling at the interface region between the piezoelectric PZT phase and the Portland cement phase. Moreover, the domain appearance of PZT can be seen to be clearer when PZT was mixed with cement and PVDF binder in the composite system.

5. The use of PVDF as a third phase and as an insulator can be seen to evidently reduce the poling time and noticeability improved the piezoelectric properties of the composites. Moreover, ε_{33} beneficially reduced as d_{33} increased giving an increase g_{33}. Therefore, this novel composite is deemed suitable for sensor application.